

Neogaeon paleomagnetism constraints on the processes at the core and surface of the Earth

D. M. Pechersky

United Institute of Physics of the Earth, Russian Academy of Sciences, Moscow, Russia

Introduction

General considerations. According to current notions, the geomagnetic field is generated by processes in the liquid core, and therefore information about its time behavior reflects the processes that occur both in the Earth's core and at its boundary with the mantle (D'' layer). On the other hand, geological information characterizes processes at the Earth's surface and in the lithosphere, and the correlation between geomagnetic and geological phenomena reflects processes in the Earth as a coherent system including core and lithosphere.

A unique source of information about the time evolution of geomagnetic field is the paleomagnetic record imprinted in ferrimagnetic minerals which are present in the majority of rocks and preserve this information over the geological history of the Earth. Available paleomagnetic data enable the analysis of geomagnetic field behavior during long time intervals. In this paper, I focus on the Neogaea, the time period covering the past 1700 Myr. I have chosen this time interval because rocks older than 2000 Ma rarely compose continuous stratigraphic sequences that were not subjected to significant transformations during their geological history and preserved the original paleomagnetic information. For this reason, we cannot now obtain an uninterrupted time series of main characteristics of the geomagnetic field and construct the geomagnetic polarity scale for the time older than 1.5–2 Ga.

Main characteristics of the geomagnetic field determined from paleomagnetic data. The geomagnetic field intensity (the vector characterized by its magnitude, direction, and time variations) is derived from both direct observations at the Earth's surface and paleomagnetic records. It is desirable to have all characteristics of geomagnetic field, but the question is which of them are actually available.

Geomagnetic **reversals**, i.e. 180° changes in the field direction, are most easily recognized. This global phenomenon underlies the construction of the global **geomagnetic polarity time scale** with the use of such methods as (1) magnetostratigraphic approach including paleomagnetic study of successive beds of stratigraphic sections, (2) magnetostratigraphic approach combining paleomagnetic determinations and radiological datings of rocks, and (3) analysis of oceanic linear magnetic anomalies.

Scale intervals are most reliable if they are constrained by all of the three methods. Since method (3) is limited by a seafloor age of 170 Ma, this interval of the geomagnetic polarity scale is most reliable.

The scale is commonly used for the analysis of the reversal frequency variation and geomagnetic polarity asymmetry over the past hundreds of millions of years (see e.g., [Algeo, 1996; Courtillot and Besse, 1987; Gaffin, 1989; Irving and Pulaiah, 1976; Johnson et al., 1995; Khramov et al., 1982; McElhinny, 1971; McFadden and Merrill, 1984, 1986; Pechersky and Didenko, 1995; Pechersky and Nechaeva, 1988]). Presently, several regional magnetostratigraphic scales have been published, providing a basis for the construction of the Neogaea polarity geomagnetic time scale [Pechersky, 1997, 1999].

The next characteristic is the magnitude of the field (intensity modulus) and its variation. The incorrect term **paleointensity**, standing for the intensity modulus, is widely accepted in the present-day paleomagnetic literature, although this term means the complete vector. Moreover, the term "paleointensity" is used even when data are given in tesla which is the measurement unit of induction. Following the "tradition", we are compelled to use the term "paleointensity" in the meaning of the paleointensity **magnitude** regardless of measurement units.

The paleointensity behavior analysis, usually including the past 400 Myr and occasionally the Phanerozoic and Proterozoic, yields evidence of preservation of the dipole field component and cyclicity of paleointensity variation close to the reversal frequency [Bolshakov and Solodovnikov, 1981; Khramov et al., 1982; Merrill and McElhinny, 1983; Pechersky, 1998; Pechersky and Nechaeva, 1988; Perrin and Shcherbakov, 1997; Petrova, 1989; Petrova et al., 1992]. The global paleointensity

database was created in the 1990s [Tanaka and Kono, 1994], which considerably stimulated the work on data generalization including the Neogaea [Pechersky, 1998].

The last characteristic is variations in the **geomagnetic field direction** at an observation point or variations in the position of the virtual geomagnetic pole (VGP), ranging within several tens of degrees. The VGP analysis can be performed only for the past few millions of years, when relative displacements of lithospheric blocks were small and VGP position may be referred to the present coordinates of an observation point.

Magnetologists often address the analysis of paleomagnetic directions and VGPs over the past 5 Myr along with data of laboratory observations (see e.g., [McElhinny and McFadden, 1997; McElhinny et al., 1996; Merrill and McElhinny, 1983; Tsunakawa, 1988]).

Information about paleointensity and field direction variations is vital to the study of the mechanism of geomagnetic field generation and development of theoretical approaches, but deep studies of the variations (and, generally speaking, the fine structure of geomagnetic field) require detailed analysis of the field behavior based on the comprehensive investigation into sections composed of rapidly accumulating volcanic-sedimentary deposits and archaeological objects. This can be done for only short time intervals because of immense volume of work and scarcity of sections that were continuously accumulated over geologically large time intervals. An alternative approach, not requiring the direct study of paleovariations of various types and origin, focuses on the analysis of the summary amplitude of all paleovariations in a given time interval, rather than the behavior of the geomagnetic field direction proper. Instead of long sections, this approach requires representative data on the concentration of paleomagnetic directions (precision parameter), because the summary amplitude of geomagnetic variations is defined by the standard angular deviation $S = 81/K^{1/2}$ where K is the precision parameter of individual vectors in terms of the spherical projection statistics [Fisher et al., 1987].

The analysis of paleomagnetic data covering geologically long time intervals was very rarely applied to the summary amplitude of Phanerozoic direction paleovariations [Irving and Pulaiah, 1976; Pechersky and Nechaeva, 1988]. The creation of the computer global database of paleomagnetic directions and poles [McElhinny and Lock, 1993] largely facilitated the problem and enabled the amplitude analysis of the Neogaea geomagnetic variation directions [Pechersky, 1996, 1997].

Cyclicity analysis. The long-period cyclicity of geomagnetic and other processes has been statistically estimated in a number of works (see e.g., [Keondzhyan and Monin, 1977; Loper et al., 1988; Marzocchi and Mu-

larga, 1992; McElhinny, 1971; Merrill and McElhinny, 1983; Pechersky and Didenko, 1995; Pechersky and Nechaeva, 1988]). Periods of about 15 to 430 Myr have been revealed. Different geomagnetic polarity regimes with characteristic times of 1, 10, 50, and 200 Myr have been recognized; they serve as a basis for the classification of magnetic zones of various ranks, their correlation and construction of magnetostratigraphic scales [Danukalov et al., 1983]. On the other hand, some authors note that no periodicity is observed in the intervals between reversals; i.e., this process is stochastic, with reversal frequency increasing in the Mesozoic-Cenozoic, and this general trend is modified by a periodicity mainly related to the thermal regime at the core-mantle boundary (in the boundary layer D'') and possibly with its topography [Cox, 1981; Gubbins, 1989; Marzocchi and Mulargia, 1992; McFadden and Merrill, 1984; Ricou and Gibert, 1997].

Correlations between geomagnetic field variations (core) and surface processes. During more than one decade, attempts have been made to generalize available paleomagnetic data and to find regularities in the behavior of main geomagnetic field characteristics and their correlations with other phenomena of the Earth and surrounding space. We dwell on examples of investigations into long-period processes.

Correlations of tectonic, magmatic, climatic, paleogeographic, and biostratigraphic events, as well as their cyclicity, with the geomagnetic field behavior and specifically with geomagnetic reversals have been noted by many authors [Aparin, 1982; Courtillot and Besse, 1987; Didenko, 1998; Eide and Torsvik, 1996; Gaffin, 1987; Khramov, 1978; Khramov et al., 1982; Kiselev and Aparin, 1987; Kravchinskii, 1977, 1987; Larson, 1991; Larson and Olson, 1991; Loper and McCartney, 1986; Loper et al., 1988; Marzocchi et al., 1992; Pechersky and Didenko, 1995; Pechersky and Nechaeva, 1988; Rampino, 1988; Rampino and Caldeira, 1993; Ricou and Gibert, 1997; Varygin and Aparin, 1989; Vogt, 1972, 1975]. This evidence supports the well-known concept of deep origin of tectonic movements and universality of the Earth's endogenic process. A pioneer of this concept was Yu. M. Sheinman. Developing the ideas of Sheinman, Kravchinskii [1977, 1987], Khramov [1978], Khramov et al. [1982], and Khramov and Kravchinskii [1984] compared the geomagnetic reversal behavior, paleomagnetic pole velocities, accelerations of continents, stages of plate subduction and obduction, stages of folding and continental basaltic volcanism (traps), seafloor accretion rate, and other events and found that events at the core and in the lithosphere correlate on a qualitative level. They concluded that global processes of the Earth are basically interrelated. Kravchinskii offered the concept of **geomonic periodicity** according to which all

events of the same rank are essentially equivalent. This leads to the **principle of conjugation** which states the possibility of sufficiently accurate quantification of one event or process in terms of another. Large-scale cyclicity has been revealed in both the geomagnetic field behavior and plate motion, and three Vendian–Phanerozoic stages are recognized in the plate configuration [Khramov, 1991; Khramov *et al.*, 1982; Zonenshain *et al.*, 1987, 1990]: (1) Late Riphean–Vendian: continents form a supercontinent (Pangea); (2) Early–Middle Paleozoic: continents are concentrated near the equator in the southern hemisphere, and plate velocities, averaging high values, considerably fluctuate; and (3) Late Paleozoic–Cenozoic: at the beginning of this stage, continents were aligned along a meridian and formed a new Pangea; plate velocities were more uniform, reaching a minimum by the middle of the stage. Later, continents resume their E–W configuration, although by that time they are mostly located in the northern hemisphere. Similar to the geomagnetic field, their main reorganizations occurred at times of ≈ 600 and 260–300 Ma. Paleomagnetic estimates of plate velocities indicate 8–10 velocity pulses in the Phanerozoic so that each two pulses form an interval nearly coinciding with a geotectonic cycle. Chronological correlation between the velocity pulses of horizontal movements and tectonic activity in the lithosphere proves that these movements are the main factor of tectogenesis [Khramov and Kravchinskii, 1984]. Moreover, the time pattern of these events, explainable within the framework of plate tectonics, is consistent with actual models of plate motion based on paleomagnetic data (see e.g., [Khramov, 1991; Khramov *et al.*, 1982; Zonenshain *et al.*, 1987, 1990]). Common periods and correlation between the events supports the concept of a global evolutionary process and general geonomic sequence of stages.

Synchronism of processes. Numerous data indicate the movements at the core–mantle boundary and in the lithosphere to be nearly synchronous. Thus, plate motion events at times of 42–45, 70–80, and 110–120 Ma were synchronous with reversal frequency changes; the stages of major changes in the biosphere and long-period variations in the seawater level, spreading rate, subduction and reversal frequency are very close in time (differing by no more than 10 Myr) [Aparin, 1982; Danukalov *et al.*, 1983; Gaffin, 1987; Loper *et al.*, 1988; McFadden and Merrill, 1986; Pechersky and Didenko, 1995; Pechersky and Nechaeva, 1988; Ricou and Gibert, 1997; Van der Voo, 1988; Vogt, 1972, 1975].

Varygin and Aparin [1989] noted a strong negative correlation of long-period variations in the seawater level with the geomagnetic reversal frequency in the Cambrian–Early Carboniferous and Late Cretaceous–Anthropogene (Marzocchi and Mulargia [1992] con-

firmed this for the past 150 Myr), whereas such a correlation is absent in the Middle Carboniferous–Early Cretaceous. In the first two periods, continents were completely isolated, and the system of mid-ocean ridges was well developed, whereas during the period with no correlation a hypsometrically high supercontinent (Pangea) existed. Supposedly, variations in the sea level give rise to small variations in geoid heights, which affect the Earth’s angular velocity and thereby the generation of geomagnetic field. Thus, the relation between variations in the reversal frequency and geoid heights (as a result of eustatic fluctuations and continental accretion processes) underlies the synchronism of global processes.

The Mesozoic–Cenozoic is characterized by synchronism between such events as trapp outflows, spreading rate jumps, stratigraphic unconformities in geological sections (reflecting eustatic sea level fluctuations), folding phases, appearance of evaporites and tillites (climatic changes), occurrence of black shales (redox conditions); their coincidence in time is most clear at 91–97, 110–113, 144–148, 190–196, and 245–250 Ma [Rampino, 1988; Rampino and Caldeira, 1993]. The cyclicity of all processes mentioned above exhibits periods approximately ranging from 20 to 100 Myr (most prominent are periods of ~ 20 –30, ~ 50 , and ~ 100 Myr).

The maximum entropy method was applied to the analysis of the Mesozoic periodicity in variations of the reversal frequency F , polarity asymmetry R , summary amplitude of direction variations S , paleointensity H_a , and continental drift velocity V [Pechersky and Nechaeva, 1988]. Mean ratios of neighboring periods of 1.4 (S), 1.67 (H_a), 1.5 (F), 1.5 (R), and 1.55 (V) are very close and similar to the ratios of short-period characteristics, which average 1.52 for two neighboring periods of secular variations and age differences of neighboring excursions [Petrova, 1989; Petrova *et al.*, 1992]. Apart from the similarity in periods, the intervals of maximum gradients of mean drift velocities virtually coincide with summary amplitude extremums of secular variations S and maximums of the R curve [Pechersky and Nechaeva, 1988].

Synchronism of geological events that occur at the surfaces of core and Earth may be due, for example, to changes in the angular velocity and/or rotation axis angle of the Earth; such changes should affect the actual motion of the geographic pole which was as large as 10–30° and more over the past 150–200 Myr [Andrews, 1985; Courtillot and Besse, 1987; Donn, 1989; Kerr, 1987; Sabadini and Yuen, 1989; Van Fossen and Kent, 1992], between the Late Ordovician and Late Devonian [Van der Voo, 1994], and in the Early Cambrian [Kirschvink *et al.*, 1997] due to both movement of mantle relative to core and rotation of the whole Earth that might be caused partly by the continental drift [Keondzhyan and

Monin, 1977]. Based on the general distribution of climates in the Phanerozoic, they came to the conclusion on systematic changes in the orientation of the Earth (relative to its axis of rotation) and in its angular velocity, caused by changes in the planetary moments of inertia due to inner redistribution of masses.

Synchronic cyclicity of many processes in the Earth, including the geomagnetic field behavior, is close to the cyclicity inherent in the tidal evolutionary scheme of the Earth–Moon system [*Avsyuk, 1986; Kiselev and Aparin, 1987*] and cyclicity of impact meteorite craters, related to the half-period of oscillations of the solar system relative to the Galaxy plane. Analyzing bio- and lithostratigraphic data associated with polarity reversal intervals, Yu. I. Kats and A. I. Bereznyakov concluded in 1974 that deceleration and acceleration stages of Earth's rotation had to give rise to geomagnetic polarity reversals, with one polarity being preferable. On a larger scale, irregular tidal slowing-down of Earth's rotation (diurnal rotation time became two times longer over the period from Archean to the present time [*Williams, 1994*]) correlates with large intervals of a constant geomagnetic polarity; thus, a departure from the monotonic slowing-down in the Late Carboniferous–Permian almost exactly coincides with the Kiaman reversed polarity superchron. Afterward the angular velocity remained nearly constant until 75 Ma when it resumed its previous value, and the second jump in the slowing-down rate occurred at the end of the Cretaceous normal polarity Djalal superchron [*Panella, 1972*]. Many authors noted the cyclicity in geomagnetic field behavior close to the galactic year [*Bolshakov and Solodovnikov, 1981; Irving and Pulaiah, 1976; Khramov et al., 1982; Loper et al., 1988; Negi and Tiwari, 1983; Pechersky and Didenko, 1995*]. Also, one should not discard the hypothesis of precession origin of geomagnetism [*Dolginov, 1977*] which provides the possibility of using the huge reservoir of Earth's rotational energy.

D'' layer and plumes. Whereas the geomagnetic field generation is associated with processes in the liquid core with characteristic times not longer than tens of thousands of years [*Merrill and McElhinny, 1983; Yanovskii, 1978*], long-period variations of geomagnetic field, which are not directly related to the core, originate at the base of the mantle (boundary layer D'') as a result of its interaction with the liquid core controlled by the heat and mass transfer between core and mantle. Temperature, density, and topography of the D'' layer are laterally inhomogeneous, and the formation of plumes may be a result of episodic instability of this layer [*Courtillot and Besse, 1987; Gubbins, 1987, 1989; Larson, 1991; Larson and Olson, 1991; Loper, 1991; Loper and McCartney, 1986; McFadden and Merrill, 1984, 1986; Stacey, 1992; Vogt, 1975; Zharkov et*

al., 1984]. The above considerations can explain the interrelation between movements in the lower mantle and surface volcanism, spreading processes (including their cyclicity), and so on. However, geochemical and seismological data indicate plumes to be formed mostly in the upper mantle at its boundary with the lower mantle, and the mass transfer between the upper and lower mantle is no more (in Cambrian even less) than 10% [*Allegre, 1997*]. Consequently, processes in the D'' layer may account for only rare large-scale tectonomagmatic events, and it is not surprising that numerous attempts were made to associate long intervals of stable geomagnetic field of constant polarity with formation of large plumes [*Courtillot and Besse, 1987; Jacobs, 1994; Larson and Olson, 1991; Loper and McCartney, 1986; McFadden and Merrill, 1984, 1996; Rampino, 1988; Vogt, 1972, 1975*]. Also, long-period variations of the geomagnetic field may be related to prolonged subduction and penetration of lithospheric cold material into the lower mantle with the formation of cold anomalies at the core boundary [*Eide and Torsvik, 1996*]. Both types of the material exchange and energy transfer (plumes and subduction) from core to surface and vice versa imply the processes at the core and Earth's surface to be recurrent. Thus, according to various estimates, the ascent of plumes from the mantle base to surface takes 10 to 40 Myr [*Courtillot and Besse, 1987; Loper, 1991; Richards et al., 1989*], which is consistent with both spreading rates and continental drift velocities [*Eide and Torsvik, 1996; Jurdy et al., 1995; Zonenshain et al., 1987*]. Lithosphere material reaches the mantle base at even smaller rates. To explain the synchronism, *Vogt* [1972, 1975] supposed a very large rate of plume ascent amounting to 1–4 m/yr. *Ricou and Gibert* [1997] note that abrupt increases in the reversal frequency and moments of major plate reorganization stages (time lags of reversal frequency peaks average 3 Myr) occurred synchronously over the past 160 Myr, which precludes the transfer of the “thermal signal” by means of mantle convection. Both events are independent and are associated with the topography of the core–mantle boundary.

Surface traces of plumes are hotspots. They are virtually immobile with respect to moving plates and spreading of oceanic lithosphere (this fact is used for reconstruction of absolute positions and motions of lithospheric plates [*Jurdy et al., 1995; Zonenshain et al., 1987*]). Therefore, processes in the D'' layer related to the formation and ascent of plumes are independent of mantle convective flows. Then, if long-period variations in the geomagnetic field are due to the processes in the D'' layer, no correlation should be expected between plate movements and motions in the layer! For example, tectonic regimes preceding the Permian–Carboniferous Kiaman and Cretaceous Djalal superchrons of constant polarity are basically different: the former took place

when continents converged to form Pangea, and the latter is associated with the time of its breakup [Eide and Torsvik, 1996].

Asynchronism of processes. Along with the synchronism, a marked time lag of 15–60 Myr is noted between the starting moments of geological epochs and increase in the reversal frequency in the Phanerozoic [Khramov *et al.*, 1982; Molostovsky *et al.*, 1976], in the Paleozoic [Didenko, 1998], and throughout the Neogaea [Pechersky, 1999], as it is mentioned above. This time lag is naturally associated with processes at the core-mantle boundary (D'' layer), and their "signals" reach the surface at the velocity close to that of the continental drift, which is probably controlled by the velocities of mantle convection and plume ascent.

Thus, at least two different, external and internal, mechanisms appear to underlie processes in the Earth. The external mechanism is responsible for synchronous processes at its core and surface, and the second one is responsible for the time lag between surface and D'' layer processes.

As it is evident from the above review, rather numerous attempts have been undertaken to generalize paleomagnetic data for studying the relationships between processes in the lithosphere and at the core. My study differs by the analysis of as many geomagnetic field characteristics as possible and encompasses a longer time interval, namely the whole Neogaea.

Part 1. Geomagnetic Field in the Neogaea

Geological Time Scale

All surface phenomena of the Earth, including geomagnetic field characteristics, are referred, one way or another, to time ("dated"). Radiometric datings bear a global character, but even they "change" with time, because decay constants are refined, new methods appear and old ones are improved, and so on. Biostratigraphic datings are less reliable and are often reasonable only on a regional scale. They need be correlated with the general geochronological scale. However, time and again this scale is improved, and paleomagnetic data obtained at various times are time correlated with somewhat different geochronological scales. Therefore, it is important to choose the scale that fixes dates for the greater part of the available information, and the remaining data should be correlated with this scale. This is the geochronological scale of Harland *et al.* [1990], with the following corrections introduced into position of boundaries in the Cambrian and Vendian [Grotzinger *et al.*, 1995] and in the Riphean [Semikhatov and Raaben, 1996]: Tremadocian, 505 Ma; Upper

Cambrian (divided into two equal intervals), 510 Ma; Middle Cambrian (divided into two equal intervals), 520 Ma; Bothomian, 525 Ma; Atdabanian, 528 Ma; Tommotian, 530 Ma; Rovenskii horizon (Nemakitian–Daldynian), 544 Ma; Kotlinskian, 551 Ma; Redkinskian, 570 Ma; Laplandian (Varanger), 610 Ma; Upper Riphean, 1050 Ma (divide into two intervals at 850 Ma); Middle Riphean, 1350 Ma (divided into two intervals at 1200 Ma); and Lower Riphean, 1650 Ma (divided into two intervals at 1450 Ma).

Of course, the scheme offered is open to criticism, but the dating accuracy of each boundary is not as important for our analysis as the correlation of the whole body of information, both paleomagnetic and geological, with one geochronological scale. (Dating uncertainties are largely reduced through smoothing.)

Geomagnetic Polarity Behavior

A composite time scale of geomagnetic polarity (Table 1) was constructed to study the polarity behavior in the Neogaea.

Geomagnetic polarity time scale. (1) The scale of Harland *et al.* [1990] was taken for times younger than 170 Ma. (2) The magnetostratigraphic scale constructed for the former USSR territory was accepted as a basis for the Paleozoic and Mesozoic time [Khramov *et al.*, 1982; Molostovsky and Khramov, 1984]. It was improved and complemented by the following regional magnetostratigraphic scales: (a) Upper Triassic–Lower Jurassic of the Newark basin [Witte *et al.*, 1991]; (b) Carboniferous of North America [Opdyke and DiVenere, 1995]; (c) Lower Carboniferous–Upper Cambrian of Ural [Danukalov *et al.*, 1983]; (d) composite magnetostratigraphic scale of the Lower and Middle Ordovician [Trench *et al.*, 1991]; (e) Ordovician–Upper Cambrian of Siberia [Gallet and Pavlov, 1996, 1999; Pavlov and Gallet, 1998]; (f) Lower Cambrian of East Siberia [Kirschvink and Rozanov, 1984]. (3) The following data were used for the Vendian and Riphean: (a) composite magnetostratigraphic scales of the Vendian–Riphean of Kuznetskii Alatau, East Siberia [Osipova *et al.*, 1988] and mid-Proterozoic supergroup, Montana and Idaho, North America [Elston and Bressler, 1980]; these scales are intercorrelated both generally and in the number of reversals; (b) Vendian section of the Pridnestrov'e area [Tretyak *et al.*, 1996]; (c) part of the Upper Riphean Katav Formation section, South Ural [Komissarova *et al.*, 1997]; (d) Mamainse Point volcanics section (Keweenawan record, Middle Riphean, 1109 to 1086 Ma) [Klewin and Berg, 1990]; (e) magnetostratigraphic section of Lower Riphean deposits, McArthur basin, Australia [Idnurm, 1992].

Younger scale intervals are naturally more reliable than older ones. Magnetostratigraphic data, obtained

Table 1. Summary Neogaeon scale of geomagnetic polarity

I	II	I	II	I	II	I	II	I	II	I	II	I	II
0.78	N	9.48	N	19.00	N	32.01	N	53.69	N	129.82	N	151.46	N
0.91	R	9.49	R	19.26	R	34.26	R	54.05	R	130.19	R	151.51	R
0.97	N	9.80	N	20.23	N	34.44	N	54.65	N	130.57	N	151.56	N
1.65	R	9.83	R	20.52	R	34.50	R	57.19	R	130.63	R	151.61	R
1.88	N	10.13	N	20.74	N	34.82	N	57.80	N	131.00	N	151.69	N
2.06	R	10.15	R	20.97	R	36.12	R	58.78	R	131.02	R	152.53	R
2.09	N	10.43	N	21.37	N	36.32	N	59.33	N	131.36	N	152.66	N
2.45	R	10.57	R	21.60	R	36.35	R	61.65	R	131.65	R	152.84	R
2.91	N	10.63	N	21.75	N	36.54	N	62.17	N	132.53	N	153.21	N
2.98	R	11.11	R	21.93	R	36.93	R	62.94	R	133.03	R	153.49	R
3.07	N	11.18	N	22.03	N	37.16	N	63.78	N	133.08	N	153.52	N
3.17	R	11.71	R	22.23	R	37.31	R	64.16	R	133.50	R	154.15	R
3.40	N	11.90	N	22.60	N	37.58	N	64.85	N	134.31	N	154.48	N
3.87	R	12.05	R	22.90	R	37.63	R	65.43	R	134.42	R	154.85	R
3.99	N	12.34	N	23.05	N	38.01	N	67.14	N	134.75	N	154.88	N
4.12	R	12.68	R	23.25	R	38.28	R	67.23	R	135.56	R	155.08	R
4.26	N	12.71	N	23.38	N	39.13	N	68.13	N	135.66	N	155.21	N
4.41	R	12.79	R	24.62	R	39.20	R	70.14	R	135.88	R	155.48	R
4.48	N	12.84	N	24.78	N	39.39	N	70.42	N	136.24	N	155.84	N
4.79	R	13.04	R	25.01	R	39.45	R	70.69	R	136.37	R	156.00	R
5.08	N	13.21	N	25.11	N	39.77	N	72.35	N	136.64	N	156.29	N
5.69	R	13.40	R	25.17	R	39.94	R	72.77	R	137.10	R	156.55	R
5.96	N	13.64	N	25.45	N	40.36	N	72.82	N	137.39	N	156.70	N
6.04	R	13.87	R	25.84	R	40.43	R	73.12	R	138.30	R	156.78	R
6.33	N	14.24	N	26.01	N	40.83	N	79.09	N	139.01	N	156.88	N
6.66	R	14.35	R	26.29	R	40.90	R	83.00	R	139.58	R	156.96	R
6.79	N	14.79	N	26.37	N	41.31	N	118.00	N	141.20	N	157.10	N
7.01	R	14.98	R	26.44	R	42.14	R	118.70	R	141.85	R	157.20	R
7.10	N	15.07	N	27.13	N	42.57	N	121.81	N	142.27	N	157.30	N
7.17	R	15.23	R	27.52	R	43.13	R	122.25	R	143.76	R	157.38	R
7.56	N	15.35	N	28.07	N	44.57	N	123.03	N	144.33	N	157.46	N
7.62	R	16.27	R	28.12	R	47.01	R	125.36	R	144.75	R	157.53	R
7.66	N	16.55	N	28.51	N	48.51	N	126.46	N	144.88	N	157.61	N
8.02	R	16.59	R	29.00	R	50.03	R	127.05	R	144.96	R	157.66	R
8.29	N	16.75	N	29.29	N	50.66	N	127.21	N	145.98	N	157.85	N
8.40	R	16.82	R	29.35	R	51.85	R	127.34	R	146.44	R	158.01	R
8.54	N	16.99	N	29.58	N	52.08	N	127.52	N	146.75	N	158.21	N
8.78	R	17.55	R	30.42	R	52.13	R	127.97	R	146.81	R	158.37	R
8.83	N	17.87	N	30.77	N	52.83	N	128.33	N	147.47	N	158.66	N
8.91	R	18.07	R	30.82	R	53.15	R	128.60	R	148.33	R	158.87	R
9.09	N	18.09	N	31.21	N	53.20	N	128.91	N	149.42	N	159.80	N
9.14	R	18.50	R	31.60	R	53.39	R	129.43	R	149.89	R	160.33	R

both before and after 1980, often do not meet the modern standard requirements of paleomagnetic reliability. There are works in which only the boundary ages of formations and other large units are reported, whereas boundary ages of magnetic zones are estimated approximately, in proportion to section thickness. For example,

such an approach was applied to age determinations of magnetic zone boundaries in sections of the Katav Formation, Lower Cambrian of Siberia, Mamainse Point, Lower Riphean deposits in the McArthur basin, and others. Some regional scales have gaps and undifferentiated intervals of frequent polarity reversals. Gaps in

Table 1. Continuation

I	II	I	II	I	II	I	II	I	II	I	II	I	II	I	II
169.11	N	250.4	N	344.0	N	410.0	N	443.5	N	516.1	N	547.0	N	1618.5	N
169.2	R	288.5	R	345.9	R	410.1	R	445.5	R	518.7	R	550.2	R	1618.8	R
169.7	N	289.0	N	347.0	N	410.2	N	448.6	N	518.9	N	554.0	N	1619.3	N
171.0	R	305.1	R	356.0	R	410.4	R	456.8	R	521.6	R	558.5	R	1619.8	R
171.7	N	305.6	N	359.5	N	410.6	N	465.0	N	521.7	N	559.0	N	1621.2	N
172.8	R	307.4	R	360.8	R	410.7	R	465.9	R	524.8	R	630.7	R	1621.5	R
176.0	N	308.2	N	361.2	N	410.9	N	467.2	N	525.0	N	634.3	N	1623.9	N
177.9	R	311.5	R	363.5	R	411.1	R	467.5	R	525.1	R	640.0	R	1624.4	R
178.7	N	312.2	N	363.8	N	411.3	N	467.7	N	525.5	N	648.6	N	1624.9	N
180.4	R	315.1	R	365.6	R	412.7	R	467.9	R	525.55	R	848.9	R	1625.1	R
182.4	N	315.3	N	366.9	N	412.9	N	468.6	N	525.65	N	863.2	N	1632.7	N
185.6	R	315.8	R	369.2	R	413.1	R	472.0	R	525.85	R	902.5	R	1633.2	R
186.3	N	316.8	N	371.5	N	413.2	N	472.3	N	526.0	N	910.4	N	1633.7	N
188.9	R	317.3	R	374.8	R	413.4	R	493.75	R	526.3	R	930.0	R	1634.3	R
199.3	N	317.7	N	376.3	N	413.5	N	496.75	N	526.6	N	931.0	N	1634.5	N
202.3	R	318.3	R	377.7	R	413.7	R	499.0	R	526.65	R	931.5	R	1634.7	R
209.3	N	320.0	N	378.4	N	413.9	N	501.5	N	527.0	N	932.0	N	1634.9	N
214.2	R	321.0	R	379.2	R	414.1	R	501.8	R	527.05	R	992.0	R	1635.4	R
214.9	N	321.5	N	380.0	N	414.2	N	502.0	N	527.15	N	1049.0	N	1635.7	N
216.5	R	321.8	R	380.8	R	416.0	R	503.6	R	527.35	R	1078.0	R	1636.1	R
217.9	N	321.9	N	384.1	N	417.2	N	504.4	N	527.4	N	1096.0	N	1638.6	N
219.1	R	322.6	R	384.9	R	419.1	R	505.9	R	527.7	R	1097.0	R	1641.5	R
220.4	N	323.3	N	385.9	N	420.4	N	506.0	N	527.8	N	1100.0	N	1655.7	N
221.0	R	323.9	R	386.6	R	420.9	R	507.8	R	528.0	R	1153.0	R	1656.2	R
222.7	N	324.6	N	386.9	N	422.0	N	508.1	N	528.05	N	1228.0	N	1657.2	N
224.2	R	325.6	R	387.8	R	424.2	R	509.2	R	528.15	R	1260.0	R	1661.1	R
225.8	N	326.7	N	388.7	N	425.8	N	509.3	N	528.4	N	1264.0	N	1661.8	N
236.0	R	330.7	R	390.8	R	428.3	R	509.35	R	528.5	R	1321.0	R	1663.0	R
241.3	N	331.6	N	392.0	N	428.8	N	509.5	N	528.6	N	1357.0	N	1663.7	N
242.1	R	332.4	R	392.6	R	429.3	R	509.8	R	528.65	R	1378.0	R	1664.0	R
242.9	N	333.2	N	393.1	N	429.5	N	510.0	N	528.75	N	1392.5	N	1666.5	N
243.4	R	333.6	R	393.9	R	429.7	R	510.3	R	528.9	R	1514.0	R	1667.9	R
244.0	N	333.9	N	394.2	N	430.1	N	510.5	N	529.5	N	1535.5	N	1682.6	N
245.0	R	334.2	R	396.6	R	430.8	R	511.7	R	529.65	R	1557.0	R	1683.1	R
245.3	N	335.0	N	399.0	N	433.2	N	511.9	N	529.7	N	1612.8	N	1683.8	N
247.0	R	335.3	R	402.5	R	434.4	R	513.1	R	529.8	R	1613.0	R	1690.8	R
247.4	N	335.9	N	404.0	N	436.8	N	513.3	N	532.9	N	1614.0	N		
248.9	R	338.9	R	405.3	R	437.7	R	514.2	R	542.0	R	1614.9	R		
249.7	N	340.2	N	405.7	N	439.3	N	514.3	N	544.0	N	1616.3	N		
249.9	R	340.8	R	406.8	R	439.7	R	514.4	R	544.7	R	1616.6	R		
250.1	N	341.4	N	409.1	N	440.8	N	514.5	N	545.0	N	1617.6	N		
250.2	R	342.8	R	409.7	R	442.7	R	515.1	R	546.6	R	1617.7	R		

I, Lower boundary of constant polarity interval (Myr). II, Polarity: N, normal; R, reversed.

the scales caused by lacking data were treated as follows: if magnetic polarities at the ends of an undocumented interval are opposite, the boundary between magnetic zones is fixed at midpoint of the interval, and if the ends have the same polarity, it is assigned to the whole inter-

val. Undifferentiated intervals of frequent polarity reversals, recognized in the Paleozoic, were treated by the following procedure. As it will be shown below, the majority of short magnetic zones in the Mesozoic and Late Paleozoic are longer than 0.25 Myr, and the undifferen-

tiated intervals were “filled” with uniformly alternating zones of normal and reversed polarities at a frequency of 2–4 reversals per 1 Myr. The composite scale was brought into correspondence with the geochronological scale (see above).

Of course, the geomagnetic polarity time scale constructed in this way (Table 1) is not free from drawbacks and is unsuitable for accurate age correlation and other magnetostratigraphic problems; moreover, it may be incomplete, particularly in the Precambrian. However, this work primarily addresses global statistical properties of the scale in order to reveal large-scale regularities and peculiarities in the geomagnetic field behavior, as well as to correlate those with other large-scale phenomena of the Earth.

I emphasize that the geomagnetic polarity time scale cannot be significantly extended into the past, because only episodically there are found rocks older than 2.0 Ga that form continuous stratigraphic sequences unaffected by significant alterations over their geological history and preserve initial paleomagnetic record.

The geomagnetic polarity time scale underlies the analysis of such paleomagnetic field characteristics as reversal frequency (Figure 1a) and polarity bias (Figure 1c).

Geomagnetic reversal frequency. To assess the reliability of the polarity time scale and related reversal pattern, relative polarity sign changes were estimated with the help of other method [McElhinny, 1971], namely from the percentage of individual paleomagnetic determinations (collections) including both field polarities with respect to their total number in a given time interval (in our case, 10 Myr, Figure 1b). This method requires statistically representative data and even in this case its results are essentially of comparative merit. In applying this method, I used the paleomagnetic database created by McElhinny and Lock [1990, 1993] and compared results with the curve constructed by the same method for the most of Phanerozoic [Johnson *et al.*, 1995]. Both curves, based on somewhat different approaches to the choice of data, virtually coincided. The Riphean section is less reliable due to long intervals for which the number of paleomagnetic determinations is less than five or they are unavailable at all.

The geomagnetic field sign patterns obtained for the Phanerozoic and Vendian by two essentially independent methods are qualitatively very similar, thereby confirming the reliability of the polarity variation (cyclicality) pattern, at least in the Phanerozoic and Vendian. Application of the two methods to the Riphean yielded differing results, which indicates the Riphean reversal pattern and Riphean interval of the polarity time scale to be incomplete [Pechersky, 1997]. For example,

marked increases in the reversal frequency obtained for the intervals 750–850 Ma, near 950 Ma, and others (Figure 1b) are not matched by a noticeable increase in the field reversal frequency in the polarity time scale (Figure 1a).

The above similarity between reversal frequency variations obtained by different methods is unrelated to their amplitudes: even in the most reliable, Cenozoic–Late Paleozoic interval of the scale (Figure 1a), the peak-to-valley value of the field reversal frequency variations as determined by the second method (Figure 1b) is several times higher than the actual value. However, their synchronism and cyclicality in the Phanerozoic–Vendian allow one to expect that the Riphean data are, on the whole, also reliable.

As it is evident from Table 1 and Figure 1, geomagnetic polarity patterns in the Phanerozoic and Precambrian are strongly different: Phanerozoic reversals were more frequent than Precambrian ones; moreover, a general increase in the number of reversals is observed: on average, one reversal occurs every 15.6 Myr in the Riphean, 1.7 Myr in the Paleozoic, 1.2 Myr in the Mesozoic, and 0.35 Myr in the Cenozoic, with long intervals of constant magnetic polarity being rather uniformly distributed throughout the Neogaea.

Magnetic polarity bias. Whereas the symmetry of magnetic hydrodynamics equations implies both polarities of the geomagnetic field to be equiprobable, intervals of dominating, normal or reversed, polarity are actually observed (Figure 1c). Importantly, the Phanerozoic polarity asymmetry derived from the geomagnetic polarity time scale coincides with the statistical estimation of the bias obtained from paleomagnetic directions of each collection included in the paleomagnetic database [Algeo, 1996], thereby confirming the reliability of the Phanerozoic polarity bias. Unfortunately, the second method fails to specify the polarity asymmetry in the Riphean, because polarity determinations are lacking for many database entries [McElhinny and Lock, 1990, 1993].

The observed complicated behavior of the polarity asymmetry cannot be explained within the framework of current dynamo models. Apparently, its origin should be sought for not in the core but in the mantle, its interaction with the core, and in external sources that change geomagnetic field generation conditions.

Duration of single-polarity magnetic zones. Histograms of magnetic zone durations (Figure 2) are generally similar for various time intervals. First, each histogram has a single mode and is close to a lognormal distribution, which indicates representativity of the Phanerozoic and Precambrian scales. Second, lengths of magnetic zones gradually increase with age, from 0.1–0.2 Myr in the Anthropogene–Miocene (Figure 2a) to

0.5–1 Myr in the time interval from the Early Mesozoic–Late Paleozoic (Figure 2d, e) through the earliest Rhiphean (Figure 2g). Therefore, magnetic zones are mostly 0.2–2.5 Myr long throughout the Neogaea and, beginning from the Late Mesozoic, gradually decreases to 0.1–0.5 Myr. This fact cannot be accounted for by systematic errors, because the mode is mostly displaced within the scale interval constructed by one method, mainly from linear magnetic anomalies in oceans (Figures 2a–2c). Third, numerous data [Petrova, 1989; Petrova and Pospelova, 1990; Petrova et al., 1992] indicate the presence of very short episodes of opposite polarities and excursions not included in the scales used for the construction of the composite Neogaeen scale. For example, the Brunhes subchron includes at least ten of such excursions. Thus, many tens of magnetic zones that are shorter than 0.01 Myr may exist; they form a separate set and have other origin. Fourth, the right-hand “tails” of the histograms disappear in the interval from the Rhiphean to Cenozoic (Figure 2): the percentage of zones longer than 5 Myr is 35% in Rhiphean, 6% in Paleozoic, and 2.6% in Late Mesozoic; in Cenozoic those are absent. Fifth, the Neogaea includes intervals dominated by one polarity as long as tens of millions of years (superchrons and hyperchrons according to magnetostratigraphic classification [Khramov et al., 1982; Molostovsky and Khramov, 1984; Molostovsky et al., 1976; Pechersky, 1985]). They are “centered” at rather regularly distributed moments of ≈ 1680 , 1520, 1360, 1150, 1100, 900, 700, 630, 470, 290, and ≈ 100 Ma spaced by about 160–200 Myr with the exception of two anomalies between 1150 and 1100 Ma and between 700 and 630 Ma (Figure 1a, b).

Thus, in view of data on excursions and short episodes, at least three field generation modes are conceivable. Fractal analysis of the scale [Pechersky et al., 1997] substantiates reliability of the above pattern (see below).

Fractal Analysis of the Reversal Scale

The case study of the geomagnetic polarity time scale over the past 170 Myr showed that the reversal sequence is aperiodic (in the strict sense of this term) and random and have fractal properties [Ermushev et al., 1992; Gafin, 1989; Ivanov, 1996; Merrill and McElhinny, 1983].

Presently, numerical modeling methods applied to the fractal sequence of geomagnetic reversals yield rather divergent results. There are models that give periodic or quasi-periodic solutions; on the other hand, Anufriev and Sokoloff [1994] obtained reversal sequences with fractal properties consistent with observations. The long Neogaeen scale allows a more detailed examination of its fractal properties [Pechersky et al., 1997].

A characteristic feature of the Neogaeen scale is the presence of constant polarity intervals whose lengths dif-

fer by more than two orders of magnitude (Table 1), which implies possible similarity between various time scales (fractality).

To study fractal properties of a geomagnetic polarity scale of length T , let N be the number of time intervals of length Δ which contain at least one reversal of the scale. The log-log dependence of $\ln N$ versus $\ln \Delta$ is a linear function whose slope is the fractal dimension d . Time series that have a constant dimension from the interval $0.5 < d < 1$ over the time period under consideration are fractal, i.e. they possess the self-similarity property.

Two linear intervals with $d_1 \approx 0.5$ and $d_2 \approx 0.87$ are recognized in the interval 170–0 Ma, with the slope of the function $N(\Delta)$ changing at about 2 Myr [Ivanov, 1996]. For the intervals 250–0 Ma (Cenozoic–Mesozoic, the scale is nearly as reliable as in the previous interval) and 560–0 Ma (Phanerozoic), the fractal characteristics remain almost the same: $d_1 \approx 0.55$ and $d_2 \approx 0.83$, and the kink is displaced toward greater Δ (Figure 3) [Pechersky et al., 1997]. Finally, if the interval 1700–0 Ma is considered, a second kink at Δ of about 50 Myr appears, and three linear segments are recognized with $d_1 \approx 0.55$, $d_2 \approx 0.66$, and $d_3 \approx 0.87$. The second kink of the function $N(\Delta)$ may be due to either (a) the fact that the Precambrian scale interval is less studied or (b) the presence of a physical process having a different fractal dimension. The following test [Pechersky et al., 1997] was performed to verify the first hypothesis: all Neogaeen intervals with $\Delta < 1$ Myr were rejected (about 20% of reversals remained), but this did not affect the position of the kink within the 1700–0 Ma interval ($d_1 \approx 0.52$ and $d_2 \approx 0.88$). Since missing reversals in the Precambrian interval of the Neogaeen scale are unlikely to exceed 80%, they cannot be responsible for the second kink in $N(\Delta)$.

To verify the second hypothesis, relatively uniform intervals with minimum reversal frequency (1600–445, 370–170, and 125–73 Ma) were chosen. Then, the remaining intervals are characterized by higher reversal frequencies, and fractal analysis was applied separately to each of the two sets. I should emphasize that each group included intervals from both the Cenozoic–Mesozoic and less reliable Early Paleozoic–Precambrian segments of the scale. Analysis of the first set yielded the $N(\Delta)$ kink at the same place as in the 1700–0 Ma variant (Figure 3) and the same dimensions of the sets $d_1 \approx 0.56$ and $d_2 \approx 0.86$. Consequently, there are no reasons to associate the fractal set with $d < 0.6$ only with high reversal frequency intervals. The second case gave a pattern very close to the 170–0 Ma variant, with $d_1 \approx 0.56$ and $d_2 \approx 0.9$ (Figure 3).

Thus, there exist three modes of the geomagnetic field generation reflected in three fractal dimensions of the reversal scale. In other words, the Neogaeen scale rep-

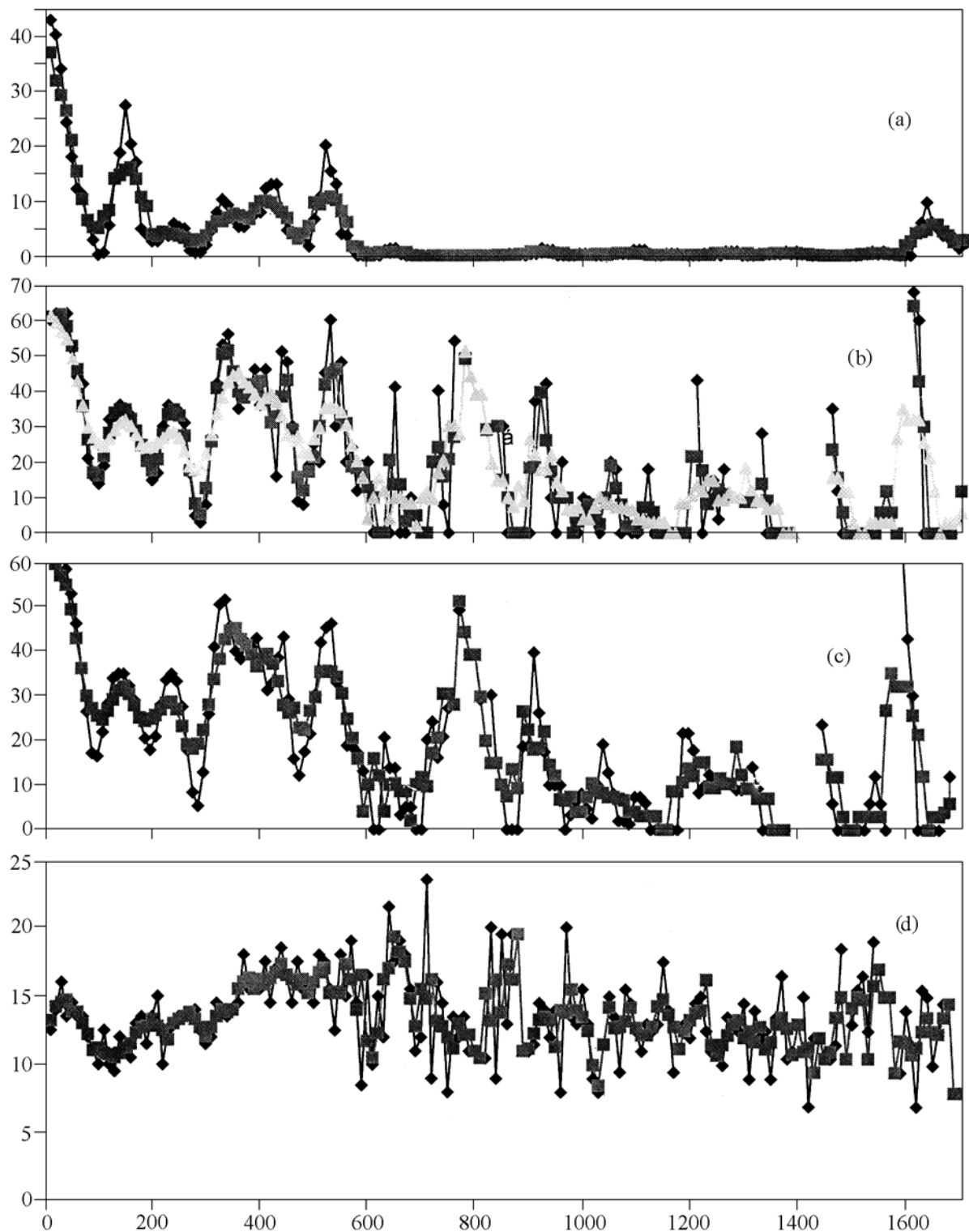


Figure 1. Variations in main characteristics of the geomagnetic field in the Neogaea: (a) reversal frequency determined from the geomagnetic polarity time scale (Table 1); (b) relative variation in the field sign, defined as the ratio of individual paleomagnetic direction determinations of a given polarity to the total number of determinations in a given time interval; (c) geomagnetic polarity bias (normal polarity percentage) determined from the polarity scale (Table 1); (d) total amplitude of direction (S) variation.

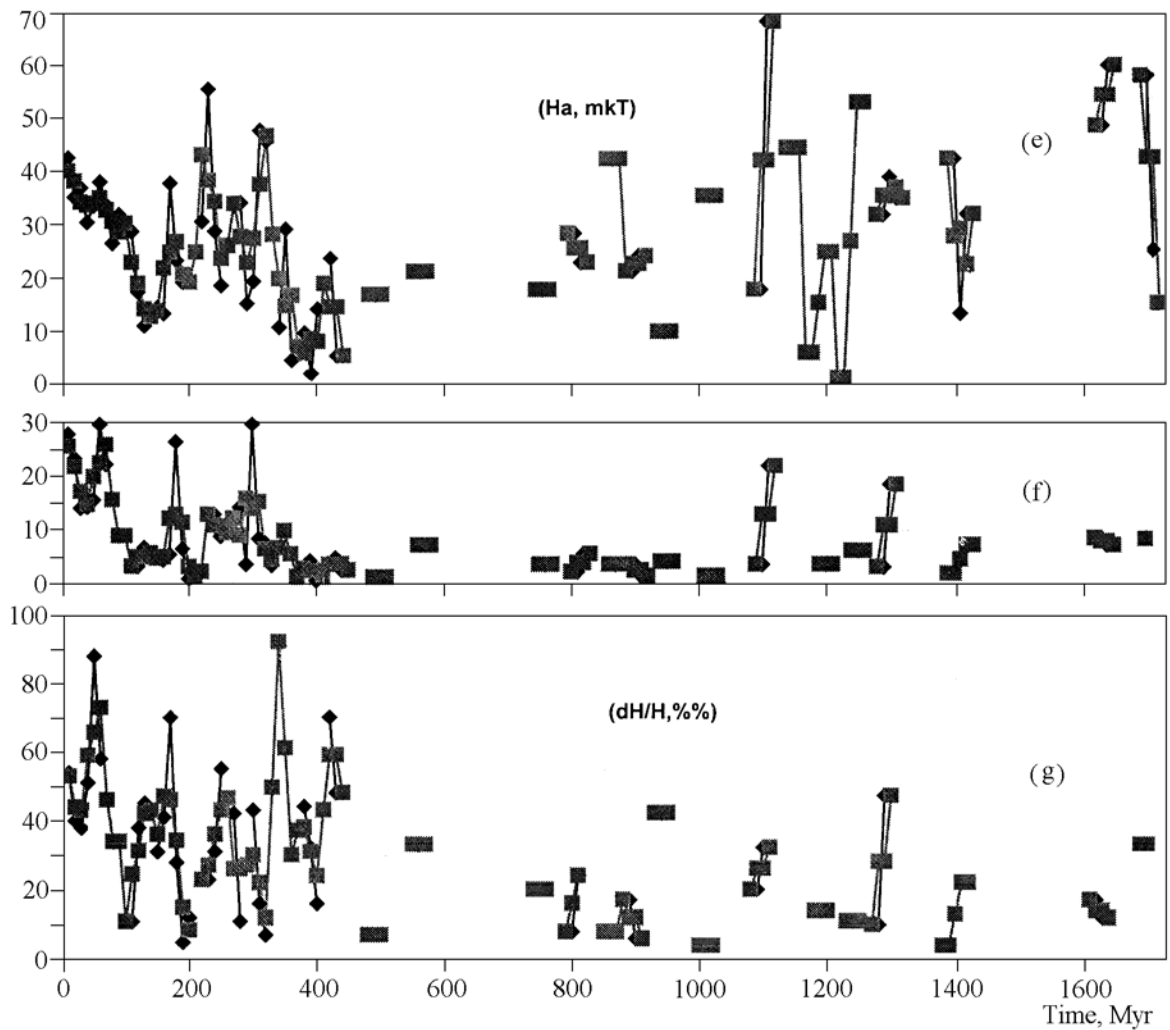


Figure 1. (Continued). (e) paleointensity modulus (H_a); (f) absolute amplitude of paleointensity variation (dH); (g) relative amplitude of paleointensity variation (dH_a/H). The plots are shown for data (1) grouped in a 10-Myr interval (diamonds) and (2) averaged over a 30-Myr interval with step of 10 Myr (squares).

resents superposition of three processes with fractal dimensions $d_1 \approx 0.56$, $d_2 \approx 0.66$, and $d_3 \approx 0.87$. The first is nearly chaotic, and the third results in concentrations (clusterization) of polarity reversals with appearance of long intervals of rare reversals; in the scale, this is reflected by regularly alternating superzones of frequent reversals (unstable field) and constant polarity (stable field). Moreover, patterns with different dimensions are superimposed, and the $d_2 \approx 0.66$ pattern may be a result of such a superposition. This is confirmed by the sample dependence of kink positions and by the fact that a gradual increase in the starting time moment does not produce in abrupt transitions between the curves $N(\Delta)$ but results in their smooth deformation associated with the lengthening of the series [Pechersky *et al.*, 1997]. Any interpretation of fractal analysis results [Anufriev and Sokoloff, 1994; Ivanov, 1996; Pechersky *et*

al., 1997] indicates the geomagnetic reversal sequence to be fractal, with a dimension d of about 0.5–0.6 and 0.9, which is conformable to the observed alternation of high reversal frequency intervals with rather long intervals of rare reversals and to chaotic distribution of reversals spaced by less than 2–3 Myr [Cox, 1981]. These regularities are observed against the background of a general increase in the reversal frequency from the Early Rhiphean to Late Cenozoic, with cyclicity of long intervals of constant polarity being on the whole preserved.

Wavelet Analysis

Fourier analysis is commonly used to reveal periodicities in a time series. However, formal application of Fourier analysis to the geomagnetic field can produce various artifacts, false periods, etc. This problem can be solved through the application of wavelet analysis

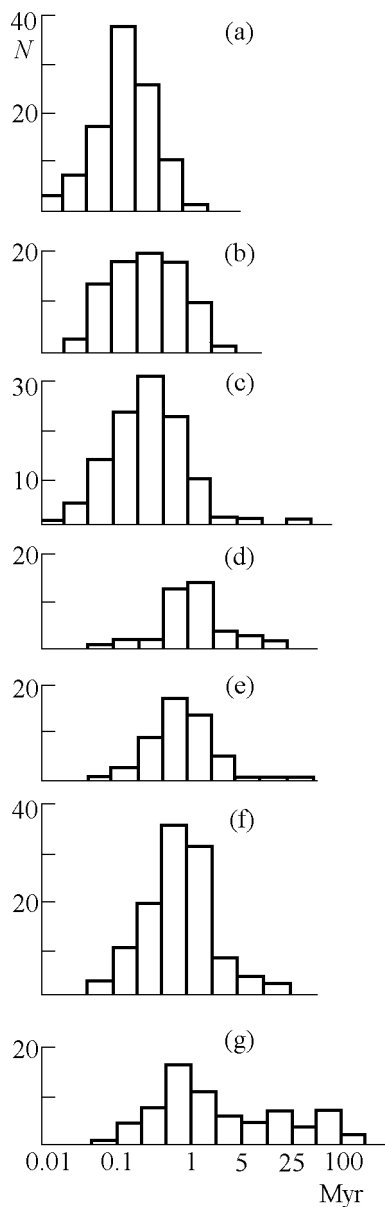


Figure 2. Magnetic zone lengths in various time intervals: (a) 23–0 Ma, Neogene; (b) 65–23.3 Ma, Paleogene; (c) 169–66 Ma, Cretaceous–Mid-Jurassic; (d) 250–169 Ma, Mid-Jurassic–Triassic; (e) 362–250 Ma, Permian–Carboniferous; (f) 545–363, Devonian–Cambrian; (g) 1700–545 Ma, Vendian–Riphean.

which compares a signal studied with a finite wave train rather than an infinite sinusoid employed in the Fourier analysis. The geomagnetic polarity time scale is described by a step function whose Fourier spectrum contains numerous multiple harmonics, whereas the wavelet analysis does not produce multiple harmonics and is efficient in studies of spectral properties of aperiodic signals [Holschneider, 1995].

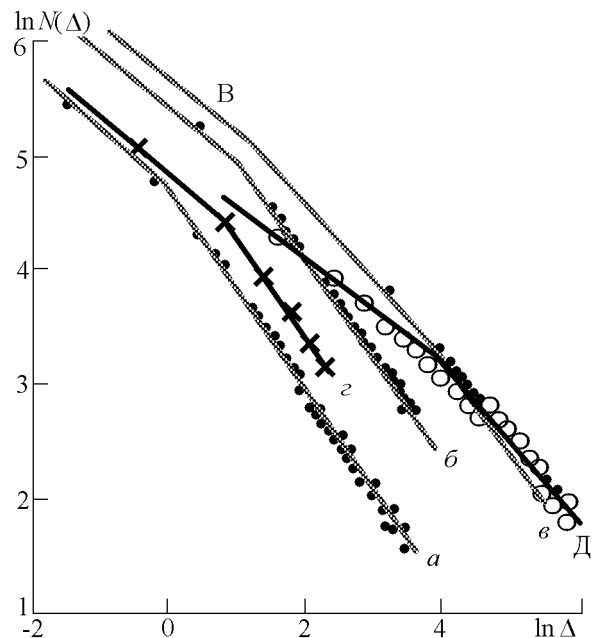


Figure 3. Fractal analysis of various Neogaeon scale intervals: (a) 170–0 Ma; (b) 560–0 Ma; (c) 1700–0 Ma; (d) intervals of frequent reversals (crosses); (e) intervals of rare reversals (circles). $N(\Delta)$ is the number of Δ -long intervals including at least one reversal.

Wavelets are a family of oscillating self-similar functions varying in scale that are localized in both physical and Fourier spaces. Wavelet analysis allows one to study spectrally nonstationary processes, examine the phase behavior of components of a quasi-periodic process, and estimate its energy characteristics. As compared with the Fourier analysis, resulting spectra are smoother and free from multiple and combination frequencies. Another advantage of the wavelet analysis is its applicability to time series with missing observations [Galyagin and Frik, 1996].

The choice of a specific wavelet depends on the purposes of analysis. In our case [Galyagin *et al.*, 1999], the Morlet and “Mexican hat” wavelets were employed. The wavelet transformation transfers a function of one variable t into the plane of two variables t and a . Here, t specifies the wavelet center position on the time axis, and the parameter a characterizes the time scale of oscillations and coincides with their period if the Morlet wavelet is used. An analogue of the Fourier spectrum is the so-called integral wavelet spectrum obtained by integration of the squared wavelet modulus along the time axis.

Wavelet analysis of the reversal frequency in the Neogaea. Periods of the integral wavelet spectrum $F(t)$ (15, 30, 50–60, 70, 100–110, 130, 180, 220,

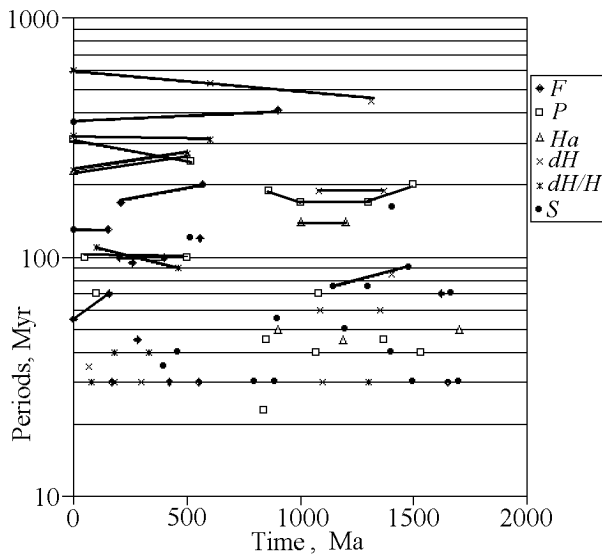


Figure 4. General cyclicity of main geomagnetic field characteristics in the Neogaea (wavelet analysis data [Galyagin *et al.*, 1999]): (1) reversal frequency F ; (2) duration of single-polarity zones (scale); (3) paleointensity H_a ; (4) paleointensity variation (standard deviation) dH ; (5) relative variation in paleointensity dH/H_a ; (6) total amplitude of field direction (S) variations.

280, and 390 Myr) are essentially the same as those previously obtained [Marzocchi and Mulargia, 1992; McElhinny, 1971; Merrill and McElhinny, 1983; Pechersky and Nechaeva, 1988]. As distinct from other methods of spectral analysis, wavelet data provide time evolution of the spectrum. We consider the Neogaeon evolution of the wavelet spectrum (Figure 4) [Galyagin *et al.*, 1999]. First, the Vendian–Phanerozoic and Riphean patterns are drastically different. Second, an oscillation with a period of about 400 Myr is recognizable throughout the Vendian–Phanerozoic interval; this period decreases from more than 450 Myr in the Vendian to less than 400 Myr in the Late Cenozoic. The lifetime of remaining oscillations with periods of 70 to 200 Myr is much shorter. Thus, oscillations with periods of 90 and 180 Myr are traceable from 550 to 200 Ma, when both periods gradually decreased from 200 to 170 Myr and from 100 to 90 Myr, respectively. A 130-Myr period is stable and exists from 180 Ma to the present time, and its resolution markedly improves toward the Cenozoic; a 70-Myr period exists from 160 Ma to the present time and decreases from 70 to 55 Myr. Third, the Phanerozoic and Early Riphean exhibit a series of “pulses” (approximately at 1650, 540, 370, and 160 Ma) at the lower boundary of the wavelet plane, which indicates their characteristic times to be about 30 Myr.

The stability of the inferred results is corroborated by their similarity for wavelet processing procedures with smoothing windows varying from 5 to 30 Myr.

Wavelet analysis of the geomagnetic polarity time scale. It is interesting to apply the wavelet analysis to the polarity scale proper [Galyagin *et al.*, 1998, 1999]. The integral wavelet spectrum is relatively smooth and exhibits one pronounced peak ($a \sim 180$ Myr) and a number of weak peaks at 12, 23, 43, 60, 100, 180, 300, and 600 Myr [Galyagin *et al.*, 1999]. The picture on the wavelet plane is considerably different from the reversal frequency spectrum (Figure 4). The oscillation with a 180-Myr period exists over the interval 1450–850 Ma. The period is 160 Myr in the middle of the interval and increases to 180–200 Myr at its ends. In the Phanerozoic, this pattern is changed by a rather stable oscillation, with its period gradually increasing from 250 to 300 Myr in the interval 450–100 Ma. The remaining “periods” observed in the integral spectrum are due to local events (pulses). Three intervals are recognized: (a) Vendian–Phanerozoic (630–0 Ma), includes five pulses, with average spacing between them being 125 Myr; (b) middle Middle Riphean–middle Late Riphean (1260–860 Ma), five pulses, average spacing of 80 Myr; and (c) Early–Middle Riphean (1670–1260 Ma), three pulses, average spacing of 140 Myr. A “quiescence” interval is confidently defined between 850 and 650 Ma (Figure 4).

Overall, wavelet planes of the polarity scale and reversal frequency (in essence, entirely different entities) yield similar evolution patterns of geomagnetic field in the Phanerozoic and Precambrian [Galyagin *et al.*, 1999].

Summary Amplitude of Paleovariations in the Geomagnetic Field Direction.

The geomagnetic polarity time scale yields evidence of the field sign, i.e. maximum changes of the field direction. The paleomagnetic database [McElhinny and Lock, 1990, 1993] provides the possibility of estimating the summary amplitude of paleovariations in the field direction, amounting to a few tens of degrees. Theoretically, the summary amplitude is defined by the standard angular deviation $S = 81/K^{1/2}$ [Fisher *et al.*, 1987; Khramov *et al.*, 1982; Merrill and McElhinny, 1983], where K is the precision parameter of individual vector directions for their normal distribution on sphere. The S value was determined in this way for the whole Neogaea [Pechersky, 1996, 1997].

Index of paleomagnetic reliability. Each paleomagnetic determination of the paleomagnetic database is characterized by its index of paleomagnetic reliability (IPR) varying from 0 to 1 and depending on the number of samples involved in a given determination, precision parameter of paleomagnetic directions, availability

of thermal and alternating field demagnetization data, paleomagnetic reliability tests (baked contact, pebble, fold, and reversal tests), quality of laboratory paleomagnetic measurements and their processing, and age determinations of rocks and stable component of natural remanent magnetization (NRM). Age determination was shown to have the greatest effect on the IPR value (particularly for Precambrian rocks) and considerably increase the scatter in S values close in age.

The IPR value was taken as a weight in the calculation of S means for each 10-Myr intervals [Pechersky, 1996, 1997]. Weighted means of S from volcanic and sedimentary rocks younger than 10 Ma do not differ on a significant level; decreasing IPR results in an increase in ΔS from 3–4° at IPR > 0.6 to 8° at IPR ≤ 0.2. Therefore, low-IPR S means may be considered reliable, which is especially important in the case of Precambrian determinations dominated by IPR ≤ 0.2.

Rock types. All rocks are subdivided into four groups according to their NRM origin: (a) volcanic rocks with the most probable primary thermal remanent magnetization (TRM); in the context of our study, the lava cooling and related acquisition of geomagnetic direction may be considered instantaneous; (b) intrusive rocks with probably dominating primary TRM; however, due to slow cooling of large bodies, variations may be averaged in a collection and even in an individual sample; (c) sedimentary rocks; they may preserve information about primary detrital remanent magnetization and exhibit marked averaging of variations within a sample due to slow deposition of sediments, postsedimentary processes, and early diagenesis; (d) “metamorphic” rocks; these are rocks that experienced various alterations, including the acquisition of a secondary, often postfolding, crystallization or chemical remanent magnetization; acquisition time of ancient magnetization in this rock group can be long, and as a result the scatter in S values is the largest. Evidently, metamorphism affects all groups of rocks, particularly ancient ones, which gives rise to a higher scatter in S values and thereby affects both the magnetization age and their relation to the variation amplitude.

Weighted averages of S insignificantly differ in young volcanic, intrusive, and sedimentary rocks, and relative variations in S , averaged over 10-Myr age intervals in the Phanerozoic and Precambrian are also similar [Pechersky, 1997]. In view of this similarity, data on all types of rocks are grouped in accordance with their IPR weight (Figure 1d). Information is irregularly distributed in time: data from the Phanerozoic are more representative, whereas Precambrian determinations are fewer, and their quality is worse (determinations with IPR ≤ 0.2 are predominant) [Pechersky, 1997].

Influence of geomagnetic reversals. To include the possible effect of transitional reversal zones, collections with a constant polarity (S_0) and those with both polarities (S_m) were separately analyzed. The probability of finding transitional-zone samples in the mixed-polarity collections was higher. Correspondingly, the S value from mixed-polarity collections of coeval rocks of one group is on average markedly higher than from single-polarity collections. This fact was accounted for through division by S_m/S_0 averaged over rocks of a given age from a given group, which reduced the scatter in data but did not affect the general behavior of S , and the Precambrian pattern became better resolved [Pechersky, 1997].

Latitude effect. To analyze the dependence of S on the determination latitude of paleomagnetic direction, the deviation of paleomagnetic latitude from its actual value should be first found. Possible underestimation of paleomagnetic latitude was analyzed using paleomagnetic data over the past 10 Myr, when the true latitude of the stable NRM component acquisition, insignificantly disturbed by lateral movement of crustal blocks, is known [Pechersky, 1996]. Mean paleolatitudes, calculated from 10° intervals of the true latitude of sampling sites for both volcanic and sedimentary rocks from mixed- and single-polarity collections, deviate from the true latitude by no more than 10°. Thus, the paleolatitude underestimation is on average insignificant.

We consider the latitude dependence of S for two main states of the geomagnetic field: (a) stable normal or reversed polarity, and (b) frequent polarity reversals [Pechersky, 1996, 1997]. Averaging data over age intervals of the stable field (Figure 5) yields the inverse latitude dependence of S close to the dipole field model of secular variations, secular variation amplitude of the present field observed in the northern hemisphere [Kono and Tanaka, 1995; McElhinny and McFadden, 1997; Pesonen et al., 1994; Yanovskii, 1978], and paleovariation amplitude in the Permian and Carboniferous, when the field was stable [Khramov et al., 1982]. This dependence is not observed during the high reversal frequency intervals (Figure 5d), which allows the following conclusions to be drawn. (1) The latitude dependence of S implies that its average value yields adequate constraints on the summary amplitude of paleovariations in the field direction. (2) Field generation conditions in the 1700-Ma interval were similar in the periods of stable (normal and reversed) polarity. (3) The summary amplitude of direction variations **did not depend** on latitude in the high reversal frequency intervals. The mean amplitude of the unstable field behavior ($S \cong 15^\circ$, Figure 5d) does not differ from the mean amplitude of the stable one near the equator (Figure 5i); therefore,

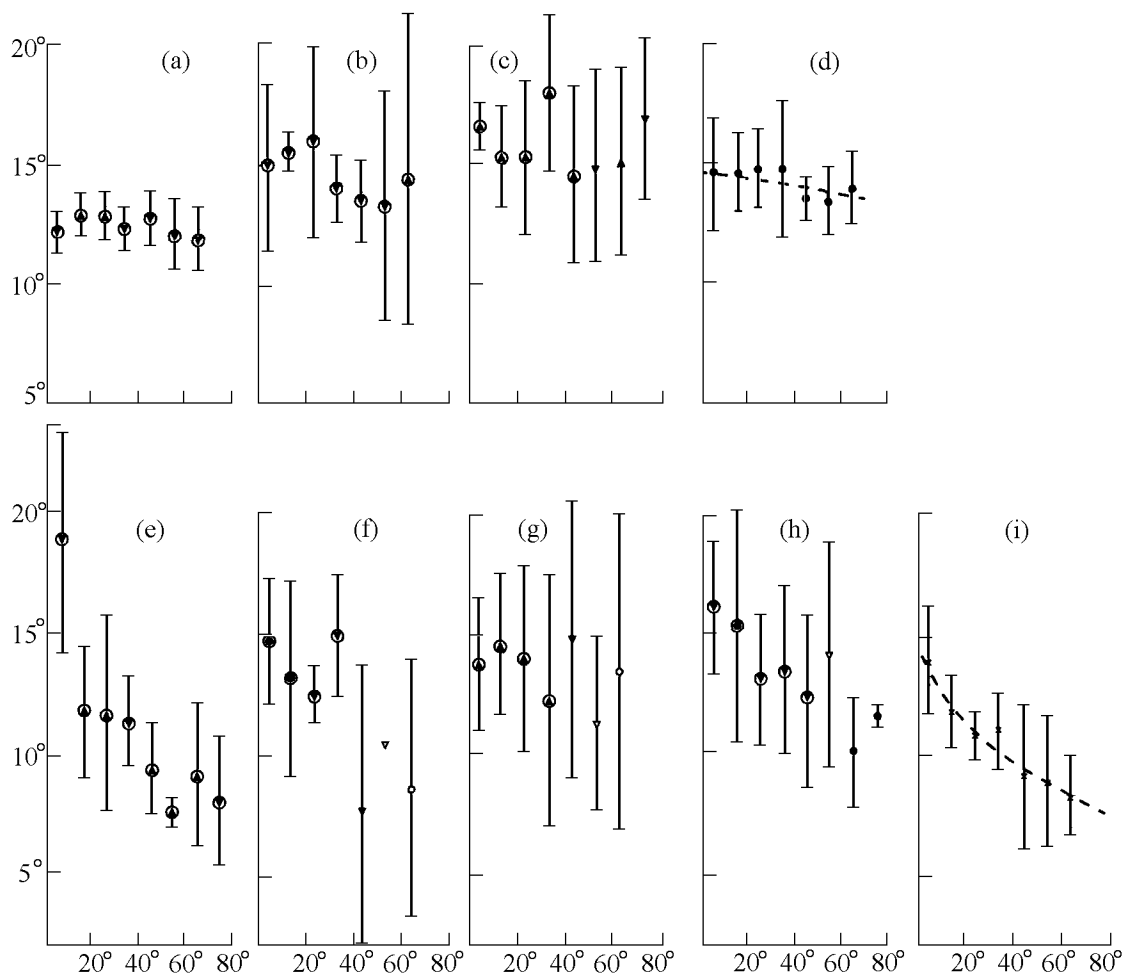


Figure 5. Latitude dependence of S for various geomagnetic field regimes. Intervals of frequent reversals: (a) 10–0 Ma; (b) 45–15 Ma; (c) 554–365 Ma; (d) averages for intervals (a)–(c). Intervals of predominant normal polarity: (e) 115–85 Ma; (f) 1040–1000, 1200–1150, and 1620–1580 Ma. Intervals of predominant reversed polarity: (g) 300–255 Ma; (h) 980–910 and 1500–1400 Ma; (i) Averages for stable field states (e)–(h). Circles, upside-down triangles, triangles, and squares are, respectively, $\text{IPR} \leq 0.2$, $0.2 < \text{IPR} < 0.4$, $0.4 \leq \text{IPR} < 0.6$, and $\text{IPR} \geq 0.6$. Open, Solid, and circled symbols correspond to the number of determinations of less than 5, 5–10, and more than 10. Vertical bars are standard deviations.

the S independence of latitude is not due to an increase in the variation amplitude that would mask S variation with latitude, but it is a regularity inherent in a specific generation mode of the geomagnetic field. The example of secular variations in the present field direction has shown that, first, their latitude dependence is markedly different in the northern and southern hemispheres [McFadden *et al.*, 1988; Merrill and McElhinny, 1983; Pesonen *et al.*, 1994]; second, the secular variation amplitude depends not only on latitude but also, to a large degree, on longitude [Shibuya *et al.*, 1995; Tsunakawa, 1988]; and, third, the field that existed at the core surface during the past 300 years includes, in addition to the dipole part, a combination of sta-

ble constant, immobile fluctuating, and drifting components [Gubbins, 1987], which markedly smooth the average latitude dependence. The above indicates that the amplitude of secular variations in the field direction is dominated by a nondipole component which strongly varies at the Earth's surface during epochs of unstable geomagnetic field behavior, whereas during stable field periods the nondipole field variations are regular and symmetrical and, as a result, evidently depend on latitude. The two types of field behavior are also recognizable from the analysis of geomagnetic polarity over the past 1700 Myr, providing an independent argument for the result derived from the study of the variation amplitude. The accuracy and representativity of data

are still insufficient for the analysis of intermediate field states between the two regimes considered above, transition time between those, and stability time intervals of each regime. The field stability intervals are likely to exist during very short times, alternating with and superimposing on one another [Pesonen *et al.*, 1994].

Thus, similar to the geomagnetic polarity behavior (Figure 1d), two intervals, Phanerozoic and Precambrian, differing in the type of variations in S are recognized, and the boundary between them lies at about 600 Ma. This may be explained in part by the amount and quality of data, but the characteristic features discussed above suggest that these two types of polarity behavior are likely to have actually existed. Irrespective of paleolatitude, the value of S very smoothly increases from 13° to 16° in a 1450–450-Ma interval and afterward gradually decreases to 12° until presently. High-frequency S fluctuations within $1-4^\circ$ occur against the background of this smooth variation in the amplitude of paleovariations.

Wavelet analysis of the summary amplitude of field direction variations [Galyagin *et al.*, 1999]. The smooth integral wavelet spectrum of the S time series exhibits weak peaks at 45, 80, 160, 300, 450, and about 1000 Myr. As it is evident from the wavelet plane (Figure 4), these periods are local maximums. The pattern is rather uniform at $a > 100$ Myr. The difference between the Phanerozoic and Precambrian generation modes is obvious at characteristic times smaller than 100 Myr: an interval of more intense Precambrian variations is observed at these times.

Variation in the Paleointensity (Modulus of the Field Intensity)

The absolute value of paleointensity is mostly determined by using heating methods (Thellier, Wilson–Burakov, van Zijl, Shaw, and others [Khramov *et al.*, 1982; Merrill and McElhinny, 1983; Pechersky, 1985]). The Thellier method with controllable mineral alterations is believed to be most reliable. In addition to determinations of the paleointensity H_a and related estimates of the magnetic dipole moment (DM) incorporated in the Database [Tanaka and Kono, 1994], we used data on the Paleozoic and Precambrian that were not included in this database [Harcombe-Smee *et al.*, 1994; Mikhailova *et al.*, 1994, 1996; Oppenheim *et al.*, 1994; Pavlov *et al.*, 1992; Starunov *et al.*, 1996; Thomas, 1993; Thomas and Piper, 1995; Thomas *et al.*, 1995; Ueno, 1995].

The H_a and DM determinations are distributed very irregularly in time. Thus, in many intervals occasionally reaching a length of 100 Myr, the determinations are absent at all (Figure 1e) [Pechersky, 1998]. Coverage of a 400–0-Ma interval (1058 determinations) is on the

whole satisfactory, whereas only 89 determinations are available for the Early Paleozoic–Precambrian. 681 of 1063 determinations from the Phanerozoic and 83 of 84 in the Riphean were made by using the Thellier method [Pechersky, 1998].

The values of paleointensity and related DM vary within a wide range, from <5 to $>100 \mu\text{T}$ (Figures 1e–1g). (The majority of $H_a > 100 \mu\text{T}$ values were obtained with the help of the Shaw method!) The scatter (standard deviation) in the H_a and DM determinations close in age was taken as a characteristic of the paleointensity variation amplitude.

Reliability index of paleointensity determination. Similar to the analysis of data on paleomagnetic directions used for the estimation of the amplitude of paleovariations, reliability indexes of paleointensity determinations (RIPs), ranging from 0 to 1, are introduced. The maximum RIP = 1 characterizes samples from baking zones and rapidly cooling lavas; maximum RIPs of 1, 0.6, 0.6, and 0.5 are given by the methods of Thellier, Shaw, Wilson–Burakov, and van Zijl, respectively; and RIP values of not more than 0.2 characterize other methods and paleointensity estimates obtained from relative values of thermoremanent magnetization (TRM) created in laboratory in a given external magnetic field and natural remanent magnetization (NRM). If data on paleomagnetic direction are unavailable, a value of 0.3 is subtracted from the pertinent RIP. RIP values reduced by 0.2–0.3 are commonly adopted for determinations made before 1970 and, finally, lower RIP values are assigned to less accurately dated determinations. Most authors assume that ages of rocks and stable natural remanence component coincide, provided the component is a primary TRM, the Database [Tanaka and Kono, 1994] provides very little information about the validity of the primary thermal origin of remanence.

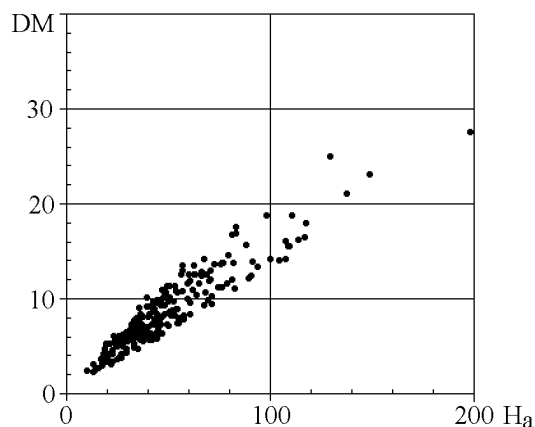


Figure 6. Plots of H_a and DM (10–0 Ma).

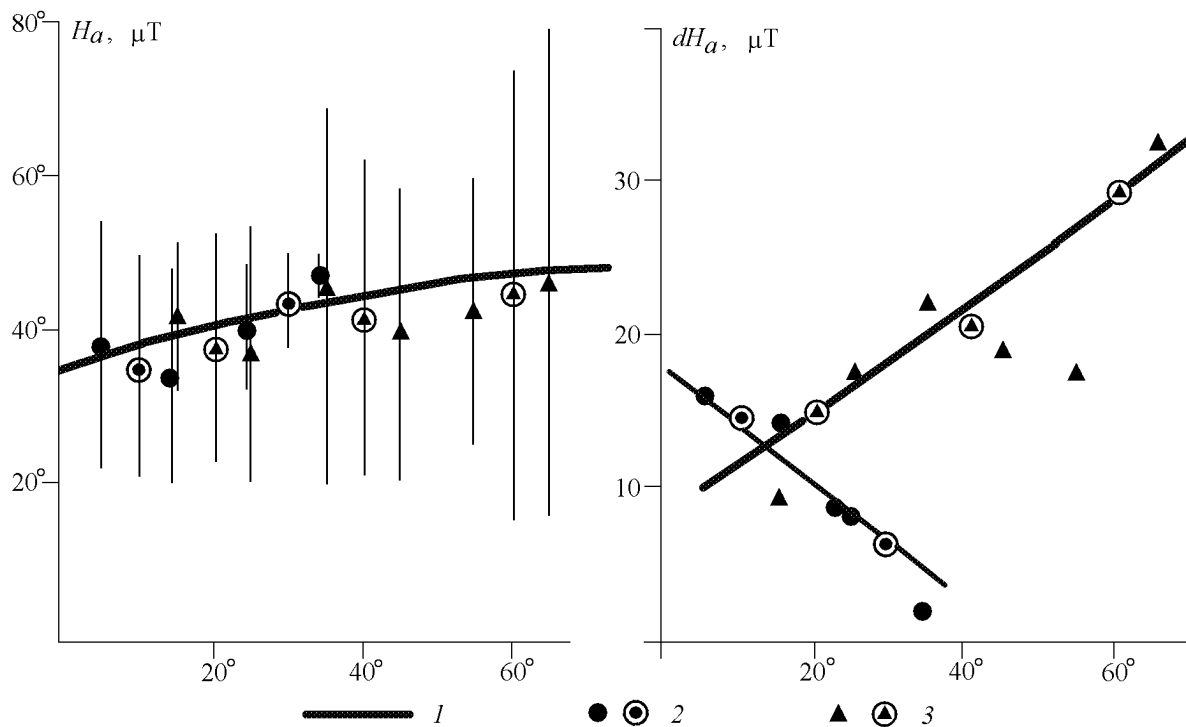


Figure 7. Latitude dependence of (a) H_a and (b) dH for two geomagnetic field regimes. (1) Central axial dipole field (Figure 7a); (2) stable polarity field (Kiaman superchron); (3) frequent-reversal field (45–0 Ma). Data are averaged over paleolatitude intervals of 10° and 20° (double circles). Vertical bars are standard deviations (dH) in a given paleolatitude interval.

Calculation of mean paleointensities includes a RIP as a weight of each determination.

The majority of determinations have $\text{RIP} \geq 0.5$ (RIPs are close to unity for many of those) mostly due to numerous Thellier determinations from baked rocks, performed by G. M. Solodovnikov and covering a 400–0-Ma interval. RIP does not exceed 0.2 in the age intervals 70–80, 170–180, 220–230, and 360–370 Ma; most Riphian determinations have $\text{RIP} = 0.4\text{--}0.5$ mainly due to lacking information about paleomagnetic directions and inaccuracy of datings [Pechersky, 1998].

The influence of geomagnetic reversals. Paleointensity is known to considerably decrease during geomagnetic reversals and excursions, but we are not interested in the field behavior during reversals. For this reason we did not consider Database determinations that were attributed by their authors to reversal zones, as well as abnormally low H_a values whose directions are untypical of their time and site.

Latitude effect. A close linear relation between H_a and DM (Figure 6) [Pechersky, 1998] reflects obvious predominance of the dipole component in H_a . The H_a value changes across the H_a (DM band by about 35%,

yielding variation in the present dipole field intensity from equator to pole. The band length which reflects the amplitude of variations in both H_a and DM considerably overlaps the possible latitude dependence of H_a .

I consider the latitude dependence of paleointensity for two cases of geomagnetic field regime: (1) unstable, with frequent reversals, and (2) stable, with very rare reversals. The time intervals 45–0 Ma and 310–260 Ma will be examined where paleointensity data are sufficiently representative and cover a wide range of paleolatitudes. In both cases, irrespective of the reversal regime, H_a averages over latitude intervals are close to the line representing the latitude dependence of field intensity of the central axial dipole (Figure 7a); therefore, the paleointensity is close to the central axial dipole irrespective of the reversal regime. The closeness of the DM to the central axial dipole is substantiated by the comparison of average DMs in the southern and northern hemispheres in the age interval 7–0 Ma. Such an interval is chosen because it is the only one in which the numbers of DM determinations in the southern (56 collections) and northern (127 collections) are more or less comparable and cover a sufficiently wide interval of latitudes. Average DMs in the northern and southern

hemispheres differ insignificantly: $(7.4 \pm 3.6) \times 10^{22}$ A m² (RIP=0.65) and $(8.5 \pm 2.7) \times 10^{22}$ A m² (RIP=0.77), respectively. To verify stability of these results, the age interval was divided into the intervals 0.9–0 and 7–1 Ma, which gave nearly the same values [Pechersky, 1998]. Thus, one may state that the geomagnetic field is close to that of a central axial dipole.

The latitude dependence of H_a variations is quite different (Figure 7b): the high reversal frequency period is characterized by an increase of the variation amplitude with latitude, which does not agree with the dipole field behavior, whereas the amplitude decreases with latitude, in accordance with the dipole field, during the stable field period.

Smoothing. To reduce the scatter in data connected with dating uncertainties and systematic errors, all results were subdivided into 10-Myr intervals in which H_a and DM averages and standard deviations dH were calculated, with weights taken in accordance with RIP indexes. The 10-Myr averages were then smoothed both with and without weighting. Smoothing windows of 30 Myr and more in length and a step of 10 Myr were used [Pechersky, 1998].

Wavelet analysis of paleointensity. In contrast to the geomagnetic polarity scale, the time series of the intensity modulus includes noticeable breaks (Figure 1) [Pechersky, 1998]. A specific wavelet analysis procedure was developed to analyze such series [Galyagin and Frik, 1996; Galyagin et al., 1999]. The integral spectrum of H_a exhibits peaks of 45, 140, 260, and 560 Myr. The wavelet plane of H_a (Figure 1) [Galyagin et al., 1999] differs from those discussed above. Only two oscillations with relatively long periods of 230–260 Myr (from about 500 Ma until present time) and 135 Myr (approximately from 1200 to 1000 Ma) are more or less reliably recognized, and a series of local maximums with periods of 30 to 80 Myr is additionally observed. Two areas of 1600–1450 and 850–450 Ma, clearly observed on the plane, are related in part to lacking data (Figure 1e); on the other hand, they resemble similar areas of other field characteristics, not related to lacking data (Figure 1). This mostly concerns the boundary region between the Riphean and Phanerozoic (circa 850–450 Ma).

Wavelet analysis of paleointensity variations. To analyze the paleointensity variation, I consider the time behavior of the standard deviation dH and ratio dH/H_a . The integral spectrum of dH is very close to the H_a spectrum and has only one additional peak yielding a period of 60 Myr. The spectrum dH/H_a is somewhat different and exhibits peaks with 40, 100, 180, 320, and 500 Myr. Like integral spectra, the wavelet spectra of H_a and dH are on the whole similar [Galyagin et al., 1999]. Thus, the higher is the intensity of an oscillation,

the stronger is its variation. The wavelet plane of dH/H_a has generally the same pattern as those of H_a and dH .

The general pattern of paleointensity behavior. The above data on the paleointensity behavior reveal three tendencies: (1) The H_a and dH scatter within comparatively narrow time limits is likely to reflect the paleointensity variation amplitude. (2) Relatively smooth long-period cyclic variations in H_a and DM are observed (with periods ranging from several tens to several hundreds of millions of years). (3) The average paleointensity level in Precambrian (DM averages 6.5×10^{22} A m²) is higher than in Phanerozoic (DM averages 4.8×10^{22} A m²); the Riphean is characterized by a general drop in paleointensity, and its general increase is observed in the Phanerozoic.

Main Features of the Geomagnetic Field Behavior in the Neogaea

1. The Neogaea is evidently dominated by the reversed geomagnetic polarity, but the normal polarity percentage increases, against the background of marked fluctuations, from the Early Paleozoic to the present time; the whole Phanerozoic is a transitional, unstable-polarity interval. This instability appears as a marked increase in reversal frequency and the shortening of single-polarity magnetic zones. The mean reversal frequency is less than 1 reversal every 10 Myr in the Precambrian (magnetic zones 1 to 100 Myr long are predominant), about 6 reversals every 10 Myr in the Paleozoic (magnetic zones 0.5 to 5 Myr long), over 8 reversals every 10 Myr in the Mesozoic (0.2 to 2.5 Myr), and about 30 reversals every 10 Myr in the Cenozoic (0.05 to 1 Myr), the frequency increasing from 12 per 10 Myr in the Early Cenozoic to 43 in the last 10-Myr interval. The aforementioned asymmetry of the field, as well as the regular distributions of its reversal frequency and lengths of constant-polarity intervals indicate that at least two field generation modes existed over the past 1700 Myr. The first mode was typical of the Precambrian and Paleozoic, when long stable-field intervals of mostly reversed polarity prevailed; the second mode characterized by frequent reversals was typical of Mesozoic and especially Cenozoic. Activities of both modes largely overlapped in time. Long stable field intervals of constant polarity were rather uniformly distributed in the Neogaea: their centers (Figure 1a, b) at about 1680, 1520, 1360, 1150, 1100, 900, 700, 630, 470, 290, and 100 Ma are spaced by 160–200 Myr except for two anomalies between 1150 and 1100 Ma and between 700 and 630 Ma, whereas the reversal frequency between these intervals considerably increases in the Phanerozoic.

The reversal sequence is fractal, with the dimensions

$d \approx 0.5$ – 0.6 and ≈ 0.9 , i.e., has the property of self-similarity of large-scale processes in accordance with the observed reversal distribution: alternation of high reversal frequency zones with fairly long intervals of rare reversals. On the other hand, their distribution within intervals of high reversal frequency is nearly chaotic ($d < 0.6$).

2. The summary amplitude behavior of field direction paleovariations is on the whole characterized by the same regularities as the reversal frequency variations; the Riphean amplitudes vary between 10° and 14° and occasionally reach 20° ; their general level weakly **rises**, whereas an inverse situation is observed in the Phanerozoic: against the background of weak fluctuations, S smoothly **falls** from 18° in the Vendian to 11° in the Cretaceous. The analysis of latitude dependence of S from three main states of the geomagnetic field (stably normal polarity, stably reversed polarity, and frequent reversals) leads to the following conclusions. (a) The variation in S with latitude implies that the paleovariations in the summary amplitude of geomagnetic field, prevailing in the Precambrian and Paleozoic, are consistent with a central axial dipole, and (b) this amplitude was on average **independent** of the paleolatitude in high reversal frequency zones. Furthermore, average amplitudes of unstable and stable regimes virtually coinciding, the invariability of S with latitude is the evidence of a different mode of geomagnetic field generation.

Mean paleolatitudes calculated from paleomagnetic inclinations provided by collections of young volcanic and sedimentary rocks of single or mixed polarity differ from the true latitude by less than 10° , which implies that, on average, the paleolatitude is not overly underestimated.

3. Three tendencies are recognizable in the intensity behavior during the Neogaea:

(a) The scatter in H_a and DM (standard deviation dH) within relatively narrow time limits is likely to reflect the amplitude of intensity paleovariations; the dH/H_a value appears to correlate with intervals of predominant reversed polarity (especially noticeable in the Riphean) and with reversal frequency.

(b) Relatively smooth long-period cyclic variations in H_a and DM are observed (over times of few tens to few hundreds of millions of years). Correlated extremums being nearly as frequent as anticorrelated ones, the time distribution of extremums of both types is rather chaotic except for the correlation between the DM and polarity asymmetry: correlation of extremums is almost everywhere normal in the Phanerozoic and inverse in the Riphean. The dH and dH/H_a values correlate with the polarity asymmetry and reversal frequency F , and the polarity asymmetry is anticorrelated with F and S in the Riphean (the correlation is mostly positive in the

Mesozoic and Cenozoic). Most noticeable is the correlation, observed throughout the Neogaea, between the lower amplitude relative variation of the paleointensity dH/H_a and Neogaeon intervals of lower frequency or absence of reversals (Figure 1).

(c) The mean level of paleointensity in the Precambrian ($DM = 6.5 \times 10^{22} \text{ A m}^2$) was higher than in the Phanerozoic ($DM = 4.8 \times 10^{22} \text{ A m}^2$); the Riphean is characterized by a general drop in the paleointensity, and the Phanerozoic, by its rise. The general Phanerozoic rise in paleointensity correlates with an increase in the summary amplitude of field direction paleovariations, in the reversal frequency, and in the percentage of normal polarity. On the whole, higher paleointensity and its smooth decrease in the Riphean correlate with the evident predominance of reversed polarity and very low reversal frequency in the same period.

The paleointensity is close to the field of a central axial dipole irrespective of the reversal regime, whereas variations in H_a show quite different latitude dependences: with increasing latitude, the amplitude of paleointensity variations increases in the case of the high reversal frequency regime and decreases in intervals of a stable field.

4. The Riphean trend of all geomagnetic characteristics changes to the Phanerozoic one at about 600 Ma.

5. Datasets providing constraints on the reversal frequency and polarity asymmetry, on dH/H_a and DM, and on S are virtually independent (this is especially true for the first two sets). This is an argument confirming the validity of the correlations between these parameters.

6. Wavelet analysis of the reversal frequency, field sign, paleointensity, variations in the field direction and intensity, and their Neogaeon evolution indicated that the geomagnetic field was generally unstable, i.e., its evolution involved no periodical processes. The following facts support this conclusion (Figure 4) [*Galyagin et al.*, 1999].

(a) A marked difference between the general patterns of wavelet spectra of all geomagnetic parameters considered above is observed. For example, if the reversal frequency F is markedly more pronounced in the Phanerozoic, the summary amplitude of variations in the field direction S , as well as change in the polarity sign P , are considerably more “active” in the Precambrian.

(b) The majority of derived periods are represented by short “events” whose length amounts to one or two full oscillations. Only four of about one hundred of such events include three to five oscillations of a given period; these are the oscillations of the reversal frequency F at a period of 100–110 Myr in the age interval from 550 to 160 Ma, oscillations of the single-polarity magnetic zone length at a period of 160–200 Myr observed from 1500 to 850 Ma, oscillations of relative variation in paleointen-

sity dH/H_a at a period of 90–100 from 450 to 100 Ma, and oscillations of the summary amplitude of variations in the field direction S at a period of 75–90 Myr from 1450 to 1150 Ma.

(c) Oscillations of various characteristics at close periods are commonly **asynchronous**. A Riphean interval of 1500 to 800 Ma is noticeable in which oscillations of field sign and paleointensity variations with close periods of 140–180 Myr are grouped. In the Vendian, they continue as oscillations of the same characteristics and reversal frequency at a period of about 220–300 Myr (Figure 4). Moreover, oscillations of F , P , dH/H_a , and S at a period of about 100 Myr are grouped in the Phanerozoic interval between 500 and 100 Ma. The remaining preferred intervals of “periods”, without regard to the occurrence time of related oscillations, are as follows: 40–45 Myr (F , P , H_a , dH , dH/H_a , S); 60–70 Myr (F , P , dH); 80–100 (F , dH/H_a , S); 130–140 Myr (F , H_a , dH); 160–180 Myr (F , P , dH/H_a , S); 250–260 Myr (H_a , dH); 300–320 Myr (dH/H_a , S); and 500–600 Myr (P , H_a , dH , dH/H_a).

(d) Oscillation periods often smoothly vary with time (Figure 4), which is largely responsible for wide ranges of periods indicated in item “c”. Most periods decrease with time concordantly with the general acceleration of the process; thus the F period falls from 100 to 85 Myr over a 470–160-Ma interval and from 70 to 60 Myr over a 150–0-Ma interval, and the S period falls from 90 to 70 Myr during the time from 1500 to 1100 Ma. The cases of an increase in periods, consistent with the slowing-down of the process are less frequent. For example, the P and dH/H_a periods increase, respectively, from 200 to 280 Myr and from 80 to 100 Myr over a 450–150-Ma interval (Figure 4).

(e) The boundary between Phanerozoic and Riphean, best expressed on the wavelet plane of reversal frequency, is recognizable in all time series (Figure 4).

7. The general behavior of main parameters of the geomagnetic field in the Neogaea (paleointensity and its variations, and summary amplitude of variations in the field direction, polarity, and reversal frequency) provides a basis for the modeling of geomagnetic field generation and characterizes processes in the core that are comparable with processes in the lithosphere and at the Earth’s surface.

Part 2. Comparison of Processes at the Core and Earth’s Surface

According to the present concept of geodynamics, processes at the Earth’s surface and in its lithosphere, mantle, and core are closely interrelated (see Introduction), which gave rise to the concept of geonomic pe-

riodicity [*Khramov and Kravchinskii*, 1984; *Kravchinskii*, 1977] stating that all phenomena of the same rank are essentially equivalent. This provides means for a quantitative description of one phenomenon or process in terms of another (conjugation principle). Unfortunately, most surface processes either cannot be quantified or available information does not embrace even the Phanerozoic. Paleomagnetic data provide the opportunity for the most complete quantitative description of the movement of large continental blocks in the Neogaea. In view of this, I addressed the best documented, measurable geological information, namely biota evolution, chronostratigraphy, and motion of continental plates. Since the frequency of geomagnetic field sign changes, predominance of one of polarities, and relative changes in paleointensity correlate with each other and are synchronous (see Figure 1, part 1; also [*Pechersky and Didenko*, 1995], we will use data on the reversal frequency which are most representative.

Changes in the Organic World and Geomagnetic Reversal Frequency

To compare the geomagnetic field behavior with changes in the organic world, I used (1) changes in the number of units in the chronostratigraphic scale (Figure 8a), (2) changes in the diversity of families of marine organisms, and (3) extinctions of marine organism families that occurred every 10 Myr (Figure 8c). The chronostratigraphic scale of *Harland et al.* [1990] with certain modifications (see Part 1) was used for the discussion of topic (1), and topics (2) and (3) will be discussed on the basis of the Phanerozoic summary presented by *Benton* [1995] (unfortunately, data on the Riphean are not so representative); only the data on marine organisms were used because they are more representative of the whole Phanerozoic. All data are correlated with the general geological time scale.

The following regularities on three time scales have been revealed.

(1) Regularity of the first order (the whole Neogaea): a sharp difference in the differentiation degree of the chronostratigraphic and magnetostratigraphic scales in the Riphean and Vendian–Phanerozoic (Figures 1 and 8), which is consistent with a rapid progress in the development of diverse life forms beginning from the Vendian–Cambrian.

(2) Regularity of the second order (geological eras): geological eras begin later than reversal frequency minimums all over the Neogaea [*Khramov et al.*, 1982; *Molostovskii et al.*, 1976; *Pechersky and Didenko*, 1995]. This delay ranging from 35 to 60 Myr (Figure 1) averages 35 ± 10 Myr, which yields 4–10 cm/yr for the energy transfer rate from the core–mantle boundary to surface, i.e., for the mantle convection velocity. This value agrees with average velocities estimated for the

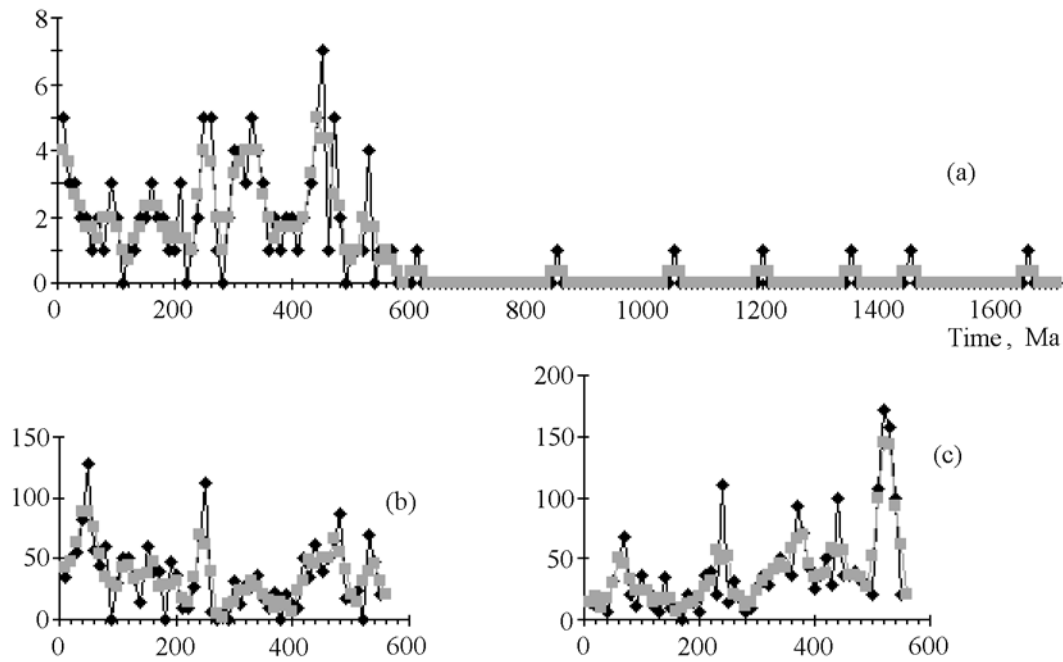


Figure 8. Variations in the organic world: (a) variations in the number of chronostratigraphic scale stages; (b) variations in the diversity of marine organism families; (c) extinctions of marine organism families every 10 Myr (after [Benton, 1995]).

drift of main continental plates (see below) [Jurdy *et al.*, 1995; Zonenshain *et al.*, 1987]. Therefore boundaries of geological eras are primarily related to an inner geodynamic mechanism.

(3) Regularity of third order (comparable with geological periods): minimums and maximums nearly coincide, which implies changes in the organic world to be synchronous with variations in the polarity reversal frequency and geomagnetic paleointensity; this synchronism is most distinct in the Phanerozoic (Figures 1 and 8). Thus, the difference between maximums (minimums) of reversal frequency and the nearest maximums (minimums) of numbers of stratigraphic units, diversity changes, and extinctions of organisms amounts to 3.1 ± 9.6 , 3.5 ± 6.3 , and 1.4 ± 9.5 Myr, respectively. Moreover, many boundaries of geological periods coincide with narrow minimums less than 10 Myr wide or with slight kinks in reversal frequency and/or paleointensity variations (Figure 1) which are smoothed away upon the 30-Myr averaging (Figure 1). Some differences in variation rates of the organic world and reversal frequency are likely to be related to deficient magnetostratigraphic information and dating uncertainties.

Thus, acceleration and deceleration of core-mantle boundary processes and evolution of the organic world occur synchronously; boundaries between geological periods are mostly associated with drops in the reversal

frequency and geomagnetic paleointensity (but not with individual reversals!) and themselves often mark a slowdown in the evolution of organic world (Figures 1 and 8).

If large long-period field variations directly affect changes in the organic world, strong (direct or inverse) correlation should exist between synchronous variations in characteristics of organic world and geomagnetic field, in particular, reversal frequency. However, numerical estimates do not confirm such a correlation, as it is evident from Figure 9. Consequently, an immediate effect of long-period field variations on changes in the organic world is either absent or insignificant, and only their cyclicities coincide.

Thus, the comparison of variation rates of organic world and geomagnetic field demonstrates that processes on a geological time scale, as well as shorter processes, which occur near the core and surface, are virtually synchronous, but they are not connected with each other or, speaking more cautiously, their interrelation is obviously secondary and not causative: the processes “respond” to a common external mechanism producing, for example, changes in the rotation axis angle and/or angular velocity of the Earth, which in turn synchronously affect movements in the core and lower mantle, producing changes in the geomagnetic field, and tectonic, climatic and other processes at the surface, producing changes in the state of biosphere. It is only

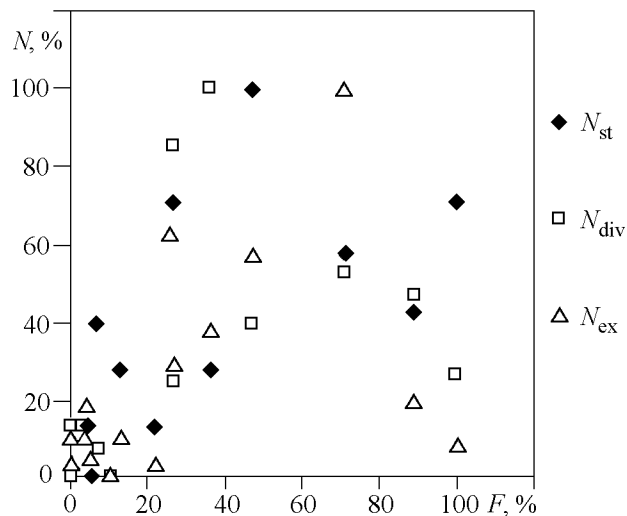


Figure 9. Synchronous relative extremums (in percent) of the number of stages (diamonds), diversity of marine organisms (squares), and their extinctions (triangles) compared with relative extremums in the geomagnetic reversal frequency. For the sake of clearness, these values are normalized to a maximum peak of a given characteristic. (a) Data are grouped in 10-Myr intervals. (b) Data are smoothed using a 30-Myr interval.

geodynamic processes on a scale of geological eras that are related to the internal mechanism of upward energy transfer from the lowermost mantle (possibly through convection, plume ascent, etc.)

Horizontal Velocities of Continental Plates

The analysis of movements of tectonic blocks usually includes the following procedures: construction of the apparent pole wander path (APWP) of a given block over a specific geological time interval from paleomagnetic directions; spatial paleoreconstructions of a block (and adjacent blocks) for various time intervals, including the positioning of Euler poles of rotation; and determination of the block velocity for various time intervals from the motion of a certain point of the block. The reconstructions are based on tectonic, paleogeographic, paleoclimatic, and other evidence, position of hotspots, and balance of forces that affect the plate motion (slab pull in subduction zones, pull-apart forces at mid-ocean ridges, etc.) [Zonenshain *et al.*, 1987]. Phanerozoic position of six continental plates (Africa, Antarctic, Europe, Siberia, India, and North America) has been recently reconstructed, and their velocities have been estimated [Jurdy *et al.*, 1995]. However, paleoreconstruction of relative and especially absolute positions of the plates are rather ambiguous (particularly in the Precambrian). This is one of reasons why paleotectonic reconstructions of continental plates are

not used here. However, the main reason is that this work addresses global regularities in tectonic motions rather than movements of separate blocks. The motion of continents across the Earth's surface resembles that of ice blocks during an ice drift: as a whole, those move downstream, although individual blocks may have different velocities, rotate in various senses and at various angular velocities, stop, and even move upstream, but the movements of each separate ice block have little in common with general regularities of the flow which are the main concern of this paper. Therefore, to simplify the problem I will consider separately the latitude (constrained by paleomagnetic inclination) and rotational (constrained by paleomagnetic declination) components of the block velocity with respect to a point in the vicinity of its center as it is readily done from its APWP. I used primarily the longest APWPs of various continental blocks, reconstructed by various authors and published reviews of paleomagnetic pole positions. The data collection included the following regions (the time series data and coordinates of the plate "center" are presented in parentheses): Australia (1700–0 Ma; 25°S, 135°E), Africa (720, 550–0 Ma; 0°S, 30°E), Europe (1700–0 Ma; 55°N, 35°E), India (1000, 820–750, 600–0 Ma; 20°N, 80°E), North America+Greenland (1300–1140, 1120–0 Ma; 40°N, 255°E), northern China (580–0 Ma; 45°N, 120°E), southern China (600–550, 450–0 Ma; 30°N, 110°E), and Siberia (1100–840, 730, 640–0 Ma; 60°N, 105°E) [Dawson and Hargraves, 1994; Elming *et al.*, 1993; Embleton, 1984; Enkin *et al.*, 1992; Gordon *et al.*, 1984; Hyodo and Dunlop, 1993; Idnurm and Giddings, 1988; Khramov, 1991; Klootwijk, 1984; Lin *et al.*, 1985; Meert and Van der Voo, 1996; Park *et al.*, 1995; Park and Gower, 1996; Pechersky and Didenko, 1995; Piper, 1995; Pisarevsky *et al.*, 1997; Radhakrishna and Joseph, 1996; Radhakrishna and Mathew, 1996; Saradeth *et al.*, 1989; Seguin and Zhai, 1992; Shapiro *et al.*, 1997; Smethurst *et al.*, 1998; Tarling and Abdel-dayem, 1996; Torsvik *et al.*, 1992; Van der Voo, 1988, 1990; Van der Voo and Meert, 1991; Wu *et al.*, 1993; Zhao *et al.*, 1990, 1993].

The data collected were revised and generalized. Paleomagnetic determinations close in age are sometimes strongly divergent and give abnormally high velocities. These are mostly data from the Early and Middle Rhiphean of Africa, India, and North America. Such intervals were rejected. Paleolatitude, paleoinclination, paleolatitude component of the plate motion velocity, and angular velocity of paleoinclination variation (rotation about a fixed point of a plate) were calculated at centers of each plate for every 10-Myr APWP interval. To remove possible errors, the results were averaged with a smoothing window of 30 Myr. These data were used for the calculation of mean paleolatitude velocities of plate motion V_{pl} (Figure 10a) and rotation V_D (Figure 10b),

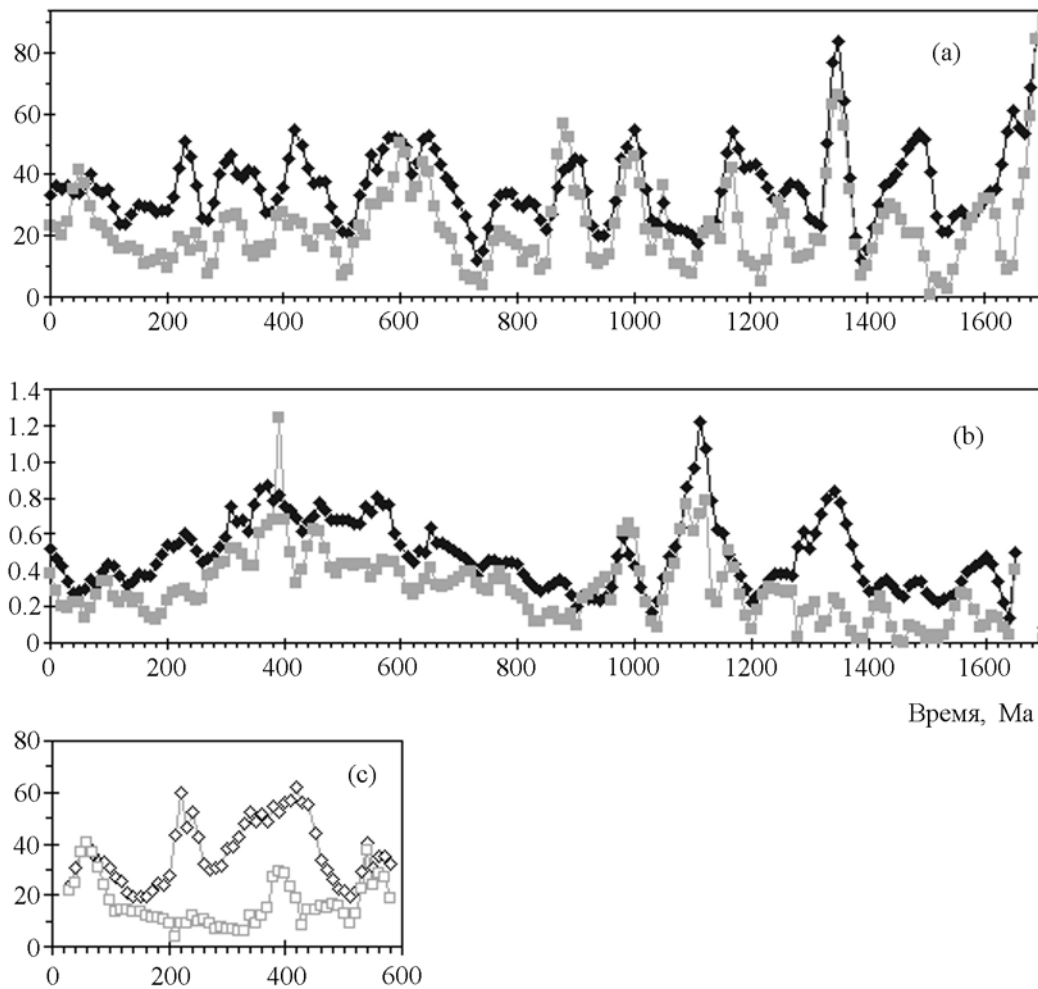


Figure 10. Mean velocities (diamonds) and their standard deviations (squares) for eight continental plates (Australia, Africa, Europe, India, North America, and northern and southern China) in the Neogaea: (a) latitude component; (b) rotation about the approximate center of plate (see Table 2); (c) motions of six continents (Africa, Antarctica, Europe, Siberia, India, and North America) after *Jurdy et al.* [1995]. The data are averaged with a window of 30 Myr and a step of 10 Myr.

as well as standard deviations from these means dV_{pl} and V_D . The means were calculated for eight plates in the Phanerozoic, five plates in the Vendian–Late Riphean, three in the Middle Riphean, and two in the Early Riphean.

The above comparison with an ice drift is clearly illustrated in Figure 11: the majority continents move, with slight variations, consistently, which is most evident beginning from the mid-Paleozoic, but opposite movements (for example, Europe, Siberia, North America, and Australia in a 1100–900-Ma interval) are also observed. The tendency mentioned in the Introduction is also evident from the figure: concentration of most continents in the equatorial zone at the time of existence

of Riphean Pangea and their divergence in the Early Paleozoic (breakup of Paleozoic Pangea) followed by movement of Laurasian continents to northern latitudes and movement of Gondwana continents to the equator and southern latitudes in the Mesozoic–Cenozoic.

The velocity pattern of the paleolatitude plate motion component is most distinct (Figure 10a), virtually coinciding with that of the full mean velocities calculated from the spatial reconstruction of Phanerozoic continents (Figure 10c) [*Jurdy et al.*, 1995], although the sets of continents (and their number) are different. Hence, V_{pl} is likely to rather adequately reflect the variation in the velocity moduli of continents in the Phanerozoic and Precambrian. Figure 10a clearly shows a cyclicity in V_{pl}

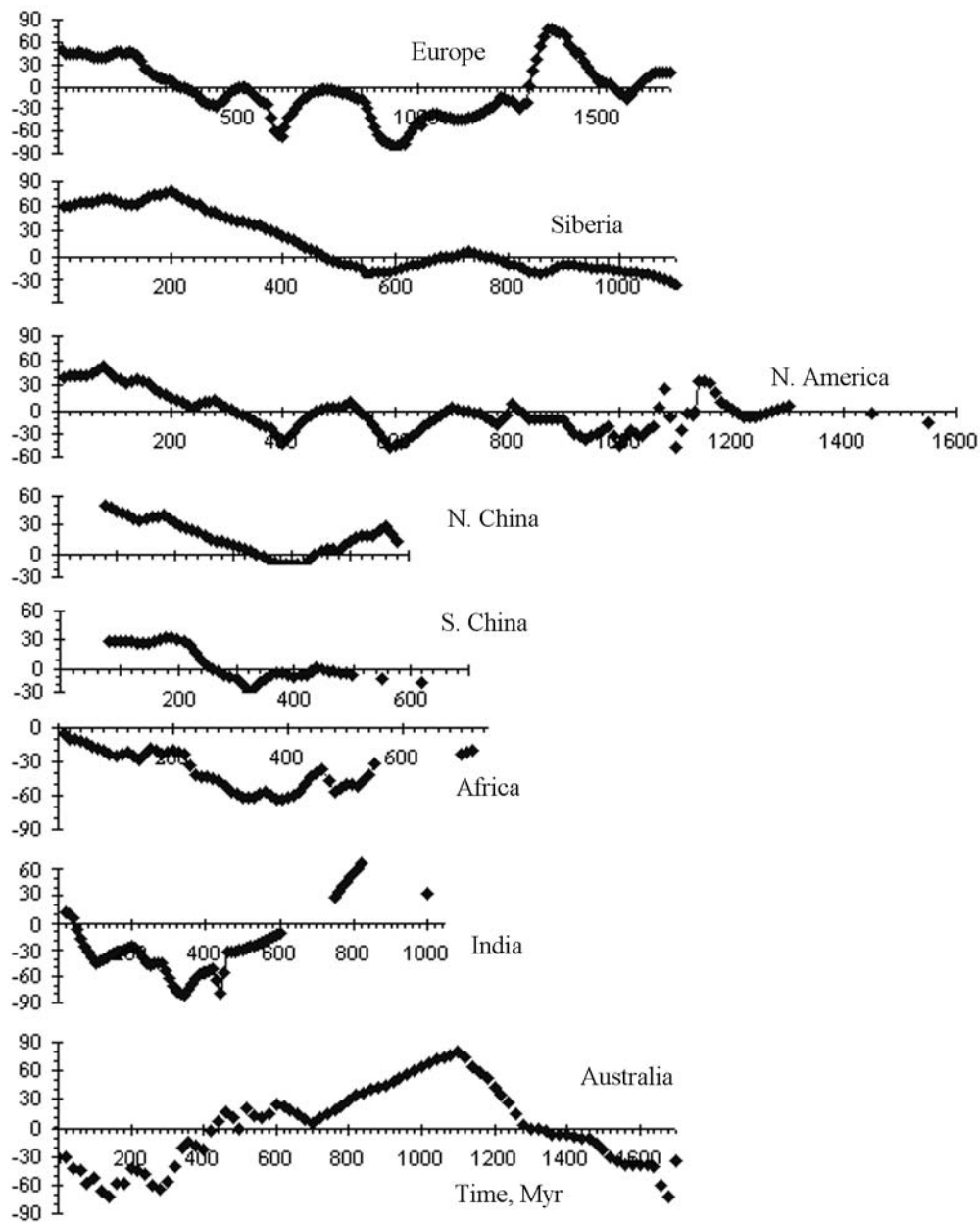


Figure 11. Paleolatitude variations of continental plates.

disturbed by less regular plate rotations (Figure 10b).

A sharp difference in the behavior of V_D and dV_D in intervals of 1700–900 and 900–0 Ma. In the first interval, V_D has a low scatter and varies rather periodically (with maximums of dV_D at 1100 and 980 Ma); in the second interval, both velocity and its scatter gradually increase toward the center of the interval and then gradually decrease. The scatters appear to be minimum during the existence of supercontinents. The V_{pl} pattern is different: its behavior, with minor deviations, is similar throughout the Neogaea and exhibits a regular change in mean velocities from their minimum (10–20 km/Myr) to

maximum (40–60 km/Myr) values rarely (in the Riphean) reaching 80 km/Myr. On the other hand, specific behavior of dV_{pl} is observed in the Riphean, where the scatter varies in the same manner as V_{pl} , and in the upper half of the Late Riphean–Phanerozoic, where their variations are different, but the most important is the relation $dV_{pl} \ll V_{pl}$. Against this background, an interval of “disturbed cyclicality” of V_{pl} and high dV_{pl} values is clearly observed in the Vendian–uppermost Riphean (650–530 Ma). Based on direct measurements of intervals between adjacent maximums (minimums) and wavelet analysis results (D. K. Galyagin and P. G. Frik),

Table 2. Comparison of APWP kinks from eight plates with the nearest reversal frequency extremums F_m

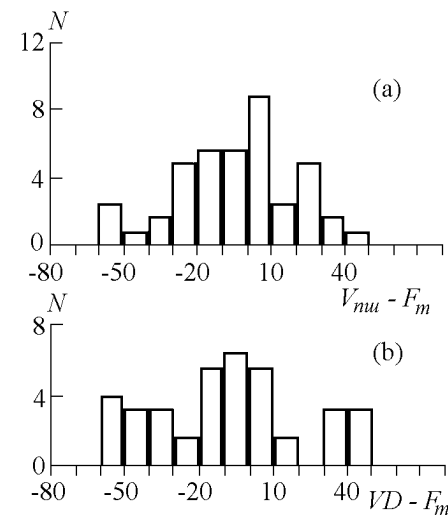
Kink age, Ma	Number of plates that have a given kink	Time between kink and F_m , Myr
65–80	8	–30, min
100–110	6	0, min
140–160	8	0, max
200–210	8	0, min
280	7	0, min
350–360	6	0, min
380–410	8	0, min ?
450	4	–20, min
480–500	4	0, min
540–560	3	–40, min
600–620	5	0, min
700	2	0, min
750	4	0, max
800	3	0, max
850	4	–20, min
1000	3	0, min ?
1050	2	0, max
1100	3	0, min
1150	2	0, min
1200	3	0, max
1300	4	0, min ?
1500–1520	2	0, min
1580	2	0, max ?
1650	2	0, min

the following characteristic times are recognized in the cyclicity of V_{pl} , dV_{pl} , V_D , and dV_D : 20–30, 40–50, 70–80, ≈ 100 , and ≈ 130 Myr.

Comparison Between Continental Plate Velocities and Geomagnetic Reversal Frequency in the Neogaea

First, I compare kinks in the plate APWPs with field reversal frequency (F) extremums (Figures 1a and 1b). As seen from Table 2, 14 kinks coincide with minimums of F , six coincide with its maximums, and four are behind F_{min} by 20–40 Myr; i.e., similar to biota variations, sharp changes in the paleomagnetic pole position are mostly synchronous with reversal frequency extremums, although there are more complex cases of delayed variations.

Now I compare the maximums (minimums) of V_{pl} , dV_{pl} , V_D , and dV_D with the closest reversal frequency maximums (minimums) of the field F_m . Unlike similar comparison with variation rates of the organic world (see above), a scatter of the extremums is broader (Fig-

**Figure 12.** Histograms of differences between adjacent maximums (minimums) of mean plate velocities and reversal frequency ($V_m - F_m$). V_{pl} for (a) the latitude component of plate velocity V_{pl} and (b) velocity of plate rotation V_D .

ure 12), which may be related to various uncertainties. The differences $V_m - F_m$ and $dV_m - F_m$ mostly form two groups: they are either close to zero (0 ± 20 Myr) or negative (mainly in the interval of -30 to -60 Myr); therefore, the velocity extremums and their scatter are either synchronous with the reversal frequency extremums or behind those by the value close to delay times of geological era onsets with respect to reversal frequency minimums (Figure 1a). In spite of a large scatter, alternation of intervals dominated by minimum differences $V_m - F_m \approx 0$ and those with the prevailing values $V_m - F_m \approx -40 \pm 20$ Myr is evident (Figure 13). The characteristic time of this alternation is 350–400 Myr.

The above data may be interpreted as evidence of two active mechanisms: the outer, operating synchronously at the core and Earth's surface, and inner, responsible for the values $V_m - F_m = -40 \pm 20$ Myr. Negative values of $V_m - F_m$ are a result of the energy transfer from the core-mantle boundary (D'' layer) to the surface (plumes, mantle convection, and so on). A delay of -40 ± 20 Myr indicates the velocity of the energy transfer to be 5–10 cm/yr. Such a velocity is consistent with Figure 8 and known estimates of mean velocities of major plates [Jurdy *et al.*, 1995; Zonenshain *et al.*, 1987, 1990].

The mechanisms may be further specified from the correlation between V_{pl} and $V_m - F_m$. If the inner mechanism is dominated by convective motions in the mantle, these values should be inversely correlated, whereas the plume mode of energy transfer probably implies such a correlation to be absent, because continental plate motions are nearly independent of the plume ascent, but they are significantly affected by convective motions in

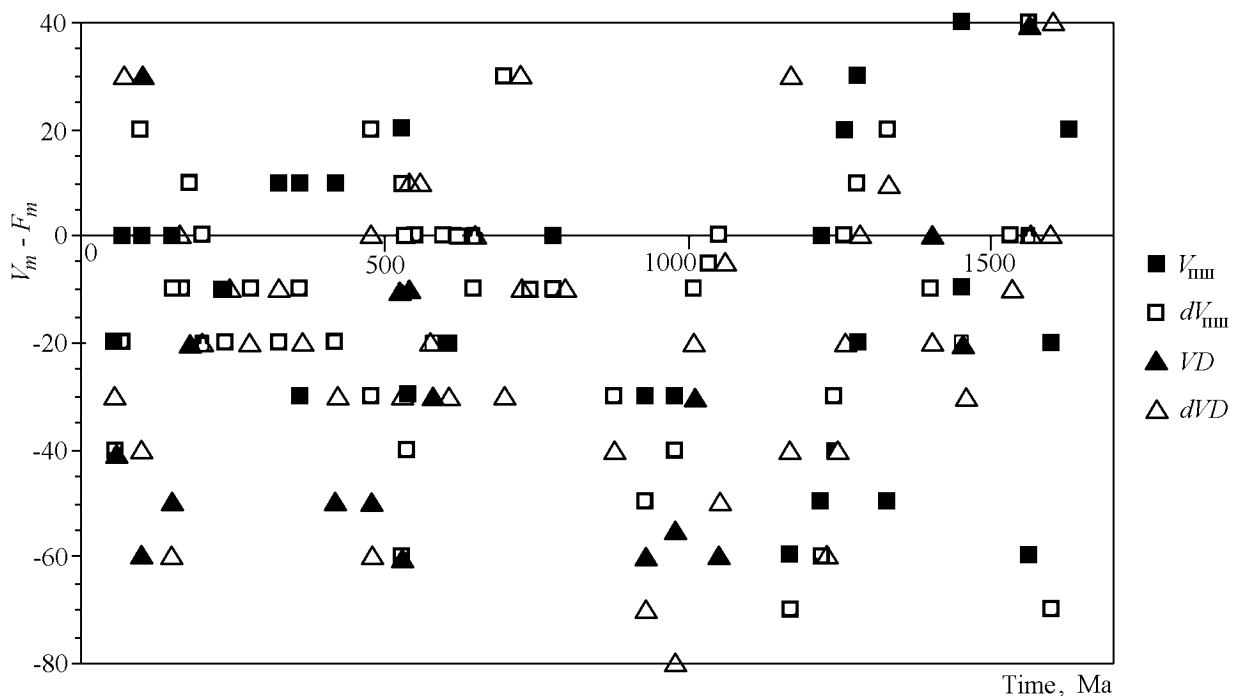


Figure 13. Differences between adjacent maximums (minimums) of mean plate velocities and reversal frequency ($V_m - F_m$). V_{pl} and dV_{pl} are the latitude component of plate velocity (solid squares) and its standard deviation (open squares). V_D and dV_D are the velocity of plate rotation (solid triangles) and its standard deviation (open triangles).

the upper mantle; no correlation should exist in the case of operation of the external mechanism. The values of V_{pl} and $V_m - F_m$ are likely to be uncorrelated in both intervals 0 ± 20 Myr and -40 ± 20 Myr (an inverse correlation seems to exist in the case of minimum values of V_{pl} , see Figure 14). Whereas the absence of correlation in a 0 ± 20 -Myr interval supports the action of the external mechanism, the absence of correlation in the second interval implies that the mantle convection is uninvolved in the interrelation between the processes in the core and lowermost mantle (D'' layer) and movements in the lithosphere. This may be explained by the fact that processes in the D'' layer and mantle convection are independent, as is indicated, for example, immobility of hotspots relative to moving plates (which is used for estimation of absolute plate movements) [Jurdy *et al.*, 1995; Zonenshain *et al.*, 1987]. The correlation may be disturbed by two-layer convection (in upper and lower mantle) which accounts for not more than 10% heat and mass transfer [Allegre, 1997].

As seen from Figures 13 and 14, the variation ranges of mean plate velocities in both mechanisms are very close (10–60 and 20–55 km/Myr) and overlap the range of possible dependence of V_{pl} on $V_m - F_m$. Therefore, the variations in the V_{pl} means are caused by general factors that affect both external and internal mecha-

nisms. The rate of core-to-surface energy transfer varies within comparatively narrow limits as is evident from a -40 ± 20 -Myr range of delay times between velocity and reversal frequency extremums and from overlapping ranges of variation in maximum and minimum values of mean velocities of paleolatitude plate movements (these ranges are, respectively, 30–60 and 10–45 km/Myr for the external mechanism and 40–55 and 20–40 km/Myr for the internal one (Figure 14). Thus, irrespective of geomagnetic field generation mechanisms and plate movements, the rates of core-to-surface energy transfer and plate motions are close, which is evidently due to properties of the medium. As seen from Figure 13, there exist time intervals dominated by the action of the external synchronous mechanism ($V_m - F_m = 0 \pm 20$ Myr) or internal mechanism with a characteristic delay time of -40 ± 20 Myr. In particular, the aforementioned Vendian interval with “anomalous” V_{pl} and dV_{pl} lies within the longest interval dominated by the action of the external mechanism (Figures 1 and 13).

Generalization of results

The above data imply that the relations between processes in the core and lowermost mantle on the one hand and at the Earth’s surface on the other hand are realized at least at three time scale levels.

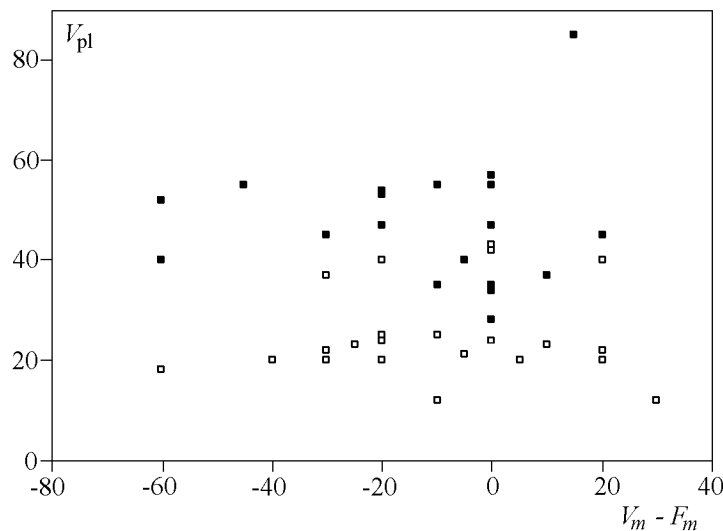


Figure 14. Maximums (solid circles) and minimums (open circles) of the latitude component of mean plate velocity V_{pl} as a function of the difference between their time and adjacent maximum (minimum) of the reversal frequency $V_m - F_m$.

First time scale level is the whole Neogaea. At the Earth's surface, a relevant characteristic feature is a different degree of differentiation of the chronostratigraphic scale in the Riphean and Vendian-Phanerozoic (Figure 8), which is evidence of an intense rise in the development of various life forms that began in the Vendian-Cambrian. The final interval of the Riphean-Vendian (650–530 Ma) is characterized by disturbed cyclicity of the continental plate velocity (V_{pl}) variation (Figure 10), and the Vendian interval of anomalous V_{pl} lies within the longest interval dominated by action of the external mechanism (Figures 1 and 13). The conclusive stage of existence of the Riphean supercontinent Pangea and its breakup also took place at that time. The peak of tectonic and thermal activity, lying approximately between 570 and 500 Ma, was associated with a higher heat flow, the widest occurrence of the granulite facies of metamorphism, reworking of the crust, and epeirogenic uplifts and basalt outflows possibly related to mantle plumes [Williams, 1994]. At the same time, essential changes at the core-mantle boundary markedly affected all characteristics of the geomagnetic field, particularly, its reversal frequency whose pattern is very close to the “frequency” of startigraphic stages (Figure 8). The geomagnetic field behavior differs in its fractality. A difference between the Riphean and Phanerozoic intervals and uniqueness of their boundary which manifested themselves at both the Earth's surface and core may be explained by resonance-type enhancement of core motions, caused by critical duration of the Earth's diurnal rotation (≈ 22.2 hours) due to the tidal decrease in its angular velocity by a factor of about 1.5

from the Archean to present time. This deceleration resulted in a considerable temperature increase near the core-mantle boundary, destabilization of the D'' layer, and ascent of mantle plumes [Williams, 1994].

Second level is the scale of geological eras, characterized by their onset delay with respect to reversal frequency minimums throughout the Neogaea. On this scale, long intervals of stable geomagnetic polarity, typically preceding the beginning of geological eras occur cyclically with a 160–200-Myr period close to the era duration (except for two anomalies between 1150 and 1100 Ma and between 700 and 630 Ma). This regularity is supported by a fractal dimension of reversal frequency of about 0.9 in the Neogaea. These stable polarity intervals are likely to coincide with plate velocity minimums, which is natural, given stable conditions at the core and Earth's surface. The aforementioned delay amounts to 35–60 Myr (Figure 1) and yields a value of 4–10 cm/yr for the energy transfer rate from the core-mantle boundary to the Earth's surface, i.e., for the mantle convection velocity. This value is consistent with mean velocity estimates for the drift of major continental plates (Figure 10) [Jurdy *et al.*, 1995; Zonenshain *et al.*, 1987]. Therefore, boundaries of geological eras are mainly related to the action of inner mechanism.

Third level is the scale of geological periods. First, it is characterized by nearly exact coincidence of minimums or maximums; i.e., variations in the organic world and continental plate velocities occur synchronously with the polarity reversal frequency and variations in

the geomagnetic paleointensity (Figures 1, 8, and 10). Moreover, geomagnetic events are synchronous with such “lithospheric” events as trap outflows, jumps in the spreading velocity, stratigraphic unconformities in geological sections (reflecting fluctuations in the sea level), folding phases, appearance of evaporites and tillites (climatic changes), occurrence of black shales (redox conditions). Most prominent is the coincidence of the above events at times of 250–245, 196–190, 148–144, 113–110, and 97–91 Ma [*Rampino*, 1988; *Rampino and Caldeira*, 1993; also see Introduction]. The cyclicity of all aforementioned processes exhibits periods ranging from 20 to 100 Myr (periods of ~ 20 – 30 , ~ 50 , and ~ 100 are best defined). In addition, many boundaries of geological periods coincide with narrow minimums less than 10 Myr long and small kinks in the reversal frequency and/or paleointensity variations (Figure 1). Consequently, accelerations or decelerations core-mantle boundary processes, variations in the organic world, plate motions, and other processes at the Earth’s surface occur synchronously, and boundaries of geological periods are often associated with a decrease in the reversal frequency and geomagnetic paleointensity and often manifest a decline in the organic world development (Figures 1 and 8).

Second, in addition to synchronism (coincidence of V_m and F_m extremums), V_m extremums are behind the reversal frequency extremums mainly by 30–60 Myr. A similar delay is observed in the onsets of geological eras with respect to reversal frequency minimums (Figures 1 and 13). Moreover, intervals dominated by the differences $V_m - F_m = 0$ alternate with those dominated by $V_m - F_m = 40 \pm 20$ Myr (Figure 13). The characteristic time of their alternation is 350–400 Myr, which is a twofold cyclicity period of constant polarity intervals.

These data may be explained in terms of active mechanisms of two types: an external mechanism that acts synchronously at the core and Earth’s surface and an internal mechanism responsible for a -40 ± 20 -Myr delay of processes at the Earth’s surface with respect to those at the core. In all of the cases, this is only a qualitative relationship, whereas no numerical relation between processes at the surface and core virtually exists (Figures 9 and 14). Consequently, there is no causal connection between these processes; rather, they are subjected to the action of a general mechanism.

The aim of this paper is to constrain current hypotheses using available information rather than to determine a specific mechanism (or mechanisms).

On one hand, there exist processes that are useful for reasonable explanation of synchronism of events at the Earth’s surface and core such as the tidal evolution of the Earth-Moon system, evolution of the Earth as a part of the Solar system, and general evolution of the Galaxy. Thus, tidal movements produce periodic variations in

the angular velocity of the Earth, Earth-Moon distance, and inclination of the rotation axis; as a result, the rotation poles of the Earth markedly change their position (rotations of the planet as a whole relative to the ecliptic and/or rotations of the mantle relative to the core). The same group of processes includes changes in the rotation axis position caused by the continental drift. The above phenomena in turn lead to changes in climate, sea level, and position of the core, which should affect the geomagnetic field. Thus deceleration-acceleration regimes of the Earth’s rotation should result in polarity reversals or preferred polarity intervals. Furthermore, the intervals of maximum gradients in mean velocities of the continental drift, summary amplitude extremums of direction paleovariations, and maximums of prevailing reversed polarity are very close to the epochs of the Solar system passage through the Galaxy plane; the main period of such oscillations is close to 30 Myr and virtually coincides with the main period of fauna extinctions, sea level lowering, large basalt outflows, folding, abrupt drops in spreading rate, and enhancement episodes of reduction conditions over the past 250 Myr [*Rampino*, 1988; *Rampino and Caldeira*, 1993], but it is also the half-period of variations in main parameters of the geomagnetic field in the Neogaea; finally, one of the periods of field characteristics and plate motions, considered above, is close to the Galactic year.

On the other hand, there are surface processes (geological era onsets, variations in mean velocities of continental plate motion, etc.) that proceed later than those at the core-mantle boundary (Figure 13); this delay is most naturally treated in terms of the energy transfer from the core-mantle boundary (D'' layer) to the Earth’s surface (plumes, mantle convection, etc.). The delay time constraint provides a value of 5–10 cm/yr for the energy transfer rate, which is consistent with velocities of major plates. Lacking (or very weak) numerical correlation implies that the mantle convection cannot be responsible for the interrelation between processes in the D'' layer and lithospheric motions. This may be explained in terms of two-layer convection (in the lower and upper mantle) with very limited heat and mass transfer between these layers (not more than 10%) [*Allegre*, 1997] and/or by the fact that processes in the D'' layer and mantle are independent.

General action of the two mechanisms may be described as follows. The external mechanism causes processes in the D'' layer (activity, instability, etc.) which stimulate the heat and mass transfer in the mantle, i.e., bring about the action of internal mechanism. Furthermore, mantle mass movements (convection, plumes, subduction), caused by the activity in the D'' layer and related to plate motions, change the planetary moment of inertia, i.e., bring about synchronous action of the external mechanism, and so on. Such a relation is sup-

ported by very close limits of variations in mean velocities of plate motion as constrained by each of the mechanisms (10–60 and 20–55 km/Myr, respectively).

In general, irrespective of mechanisms responsible for the geomagnetic field generation and plate movements, the energy transfer from the core to Earth's surface and plate movements have close velocities, so that these processes are evidently controlled by properties of the medium.

Conclusion

Main conclusions which follow from the analysis of the geomagnetic field behavior during the Neogaea and its relation to processes at the Earth's surface were stated at the end of the first and second sections. Here, restricting myself to a general consideration, I do not offer hypothetical mechanisms common to processes at the core and Earth's surface, especially as the mechanism of a (paleo)magnetic record (magnetic tape recorder) and its "author" (age and other characteristics of operator) cannot be directly determined. One may definitely state that long processes (tens and hundreds million years) at the core and Earth's surface are causally not related but are controlled by a mechanism (mechanisms) common to these processes, which occur either synchronously (external mechanism) or asynchronously (internal mechanism). One may suggest a combined action of both mechanisms: the external mechanism bring about processes in the D'' layer (activity, instability, etc.), which in their turn stimulate heat and mass transfer in the mantle, controlled by the internal mechanism. Mantle mass movements (convection, plumes, subduction) induced by the D'' layer activity are related to the drift of continents and thereby change the planetary moment of inertia, which again stimulates the synchronous action of the "external" mechanism, and so on. Such a scheme accounts for the long-period cyclicity and interrelation of processes.

Acknowledgement. This work was supported by the Russian Foundation for Basic Research, project no. 96–05–64118.

References

- Algeo, J., Geomagnetic polarity bias patterns through the Phanerozoic, *J. Geophys. Res.*, *101*, 2785–2814, 1996.
- Allegre, C. J., Limitation on the mass exchange between the upper and lower mantle: the evolving convection regime of the Earth, *Earth Planet. Sci. Lett.*, *150*, 1–6, 1997.
- Andrews, J. A., True polar wander: an analysis of Cenozoic and Mesozoic paleomagnetic poles, *J. Geophys. Res.*, *90*, 7737–7750, 1985.
- Anufriev, J. A., and Sokoloff, D., Fractal properties of geodynamo model, *Geophys. Astrophys. Fluid Dynam.*, *74*, p. 207, 1994.
- Aparin, V. P., Variations in volcanic activity and continental plate velocities in the Phanerozoic, *Dokl. Akad. Nauk SSSR*, *284*, 78–81, 1982 (in Russian).
- Avsyuk, Yu. N., An oscillatory component in the evolution of the Earth–Moon system and its comparison with geological processes in the Phanerozoic, *Dokl. Akad. Nauk SSSR*, *287*, 1097–1100, 1986 (in Russian).
- Benton, M. J., Diversification and extinction in the history of life, *Science*, *268*, 52–58, 1995.
- Bolshakov, A. S., and Solodovnikov, G. M., Geomagnetic field intensity over the past 400 Myr, *Dokl. Akad. Nauk SSSR*, *260*, 1340–1343, 1981 (in Russian).
- Cox, A., A stochastic approach towards understanding the frequency and polarity bias of geomagnetic reversals, *Phys. Earth Planet. Inter.*, *24*, 178–190, 1981.
- Courtillot, V., and Besse, J., Magnetic field reversals, polar wander, and core–mantle coupling, *Science*, *237*, 1140–1147, 1987.
- Danukalov, N. F., Kondruchina, L. S., and Chernikov, A. P., *Paleozoic paleomagnetism of the South and Central Urals*, BF AN SSSR, Ufa, 1983 (in Russian).
- Dawson, E. M., and Hargraves, R. B., Palaeomagnetism of Precambrian dike swarms in the Harohalli area, south of Bangalore, India, *Precamb. Res.*, *69*, 157–167, 1994.
- Didenko, A. N., Paleozoic 100-Myr variations in processes in the core and lithosphere, *Fiz. Zemli*, (5), 1998 (in Russian).
- Dolginov, Sh. Sh., Magnetism of planets, *Geomag. Aeron.*, (19), 569–595, 1977.
- Donn, W. I., Paleoclimate and polar wander, *Palaeogeogr. Palaeoclimat. Palaeoecol.*, *71*, 225–236, 1989.
- Eide, E. A., and Torsvik, T.H., Paleozoic supercontinental assembly, mantle flushing, and genesis of the Kiaman superchron, *Earth Planet. Sci. Lett.*, *144*, (3–4), 389–402, 1996.
- Elming, S., Pesonen, L. J., Leino, M. A. H., Khramov, A. N., Mikhailova, N. P., Krasnova, A. F., Mertanen, S., Bylund, G., and Terho, M., The drift of the Fennoscandian and Ukrainian shields during the Precambrian: a palaeomagnetic analysis, *Tectonophysics*, *223*, 177–198, 1993.
- Elston, D. P., and Bressler, S. L., Paleomagnetic poles and polarity zonation from the Middle Proterozoic Belt Supergroup, Montana and Idaho, *J. Geophys. Res.*, *85*, 339–355, 1980.
- Embleton, B. J., Continental palaeomagnetism, *Phanerozoic Earth history of Australia*, Veevers, J. J., Ed., Clarendon, Oxford, pp. 11–16, 1984.
- Enkin, R., Yang, Z., Chen, Y., and Courtillot, V., Paleomagnetic constraints on the geodynamic history of China from the Permian to the Present, *J. Geophys. Res.*, *97*, 13,953–13,989, 1992.
- Ermushev, A. V., Ruzmaikin, A. A., and Sokolov, D. D., A fractal nature of a sequence of geomagnetic reversals, *Magnetic hydrodynamics*, *4*, p. 8, 1992 (in Russian).
- Fisher, N. I., Lewis, T., and Embleton, B. J., *Statistical analysis on spherical data*, Cambr. Univ. Press, Cambridge, 1987.

- Gaffin, S., Phase difference between sea level and magnetic reversal rate, *Nature*, *239*, 816–819, 1987.
- Gaffin, S., Analysis of scaling in the geomagnetic polarity reversal record, *Phys. Earth Planet. Inter.*, *57*, p. 284, 1989.
- Gallet, Y., and Pavlov, V., Magnetostratigraphy of the Moyero river section (northwestern Siberia): constraints on geomagnetic reversal frequency during the early Palaeozoic, *Geophys. J. Int.*, *125*, 95–105, 1996.
- Gallet, Y., and Pavlov, V. E., Magnetostratigraphy of the Kulyumbe River key section, northwestern Siberian platform, *Fiz. Zemli*, 1999 (in print).
- Galyagin, D. K., and Frik, P. G., Adaptive wavelets: An algorithm for spectral analysis of signals with missing data, *Mathematical modeling of systems and processes*, (4), p. 10, 1996 (in Russian).
- Galyagin, D. K., Reshetnyak, M. Yu., Pechersky, D. M., Sokolov, D. D., and Frik, P. G., Wavelet analysis of the geomagnetic field in the Neogaea, *Fiz. Zemli*, 1999 (in print).
- Galyagin, D. K., Reshetnyak, M. Yu., Sokolov, D. D., and Frik, P. G., Scaling of the geomagnetic field and geomagnetic polarity scale, *Dokl. Ross. Akad. Nauk*, *1*, p. 1, 1998 (in Russian).
- Gordon, R. J., Cox, A., and O'Hara, S., Paleomagnetic Euler poles and the apparent polar wander and absolute motion of N. America since Carboniferous, *Tectonics*, *3*, 499–537, 1984.
- Grotzinger, J. P., Bowring, S. A., Saylor, B. Z., and Kaufman, A. J., Biostratigraphic and geochronologic constraints on early animal evolution, *Science*, *270*, 598–604, 1995.
- Gubbins, D., Mechanism for geomagnetic polarity reversals, *Nature*, *326*, 167–169, 1987.
- Gubbins, D., Implications of geomagnetism for mantle structure, *Phil. Trans. R. Soc. Lond.*, *A328*, 365–375, 1989.
- Harcombe-Smee, B. J., Piper, J. D. A., Rolph, T. C., and Thomas, D. N., A palaeomagnetic and palaeointensity study for the Permo-Carboniferous reversed superchron: the Mauchline lavas, southwest Scotland, *Phys. Earth Planet. Inter.*, *94*, 63–73, 1994.
- Harland, W. B., Armstrong, R., Cox, A., Smith, A., and Smith, D., *A geologic time scale*, Cambr. Univ. Press, New York, 1990.
- Holschneider, M., *Wavelets: An analysis Tool*, Oxford Univ. Press, Oxford, 1995.
- Hyodo, H., and Dunlop, D., Effect of anisotropy on the paleomagnetic contact test for a Grenville Dike, *J. Geophys. Res.*, *98*, 7997–8017, 1993.
- Idnurm, M., Paleomagnetism delivers a “whopper” on the southeastern McArthur Basin, *AGSO Res. News.*, *17*, 132–138, 1992.
- Idnurm, M., and Giddings, J. W., Australian Precambrian polar wander: a review, *Precamb. Res.*, *40/41*, 61–88, 1988.
- Irving, E., and Pulaiah, G., Reversals of the geomagnetic field, magnetostratigraphy and relative magnitude of paleosecular variation in the Phanerozoic, *Earth Sci. Rev.*, *12*, 35–64, 1976.
- Ivanov, S. S., Multifractal properties and the dimension of an attractor of geomagnetic field reversals, *Geomagn. Aeron.*, *36*, 149–156, 1996 (in Russian).
- Jacobs, J. A., *Reversals of the Earth's magnetic field*, Cambr. Univ. Press, Cambridge, 1994.
- Johnson, H. P., Van Patten, D., Tivey, M., and Sager, W. W., Geomagnetic polarity reversal rate for the Phanerozoic, *Geophys. Res. Lett.*, *22*, 231–234, 1995.
- Jurdy, D. M., Stefanick, M., and Scotese, C. R., Paleozoic plate dynamics, *J. Geophys. Res.*, *100*, 17,965–17,975, 1995.
- Keondzhyan, V. P., and Monin, A. S., On the pole wander caused by the drift of continents, *Dokl. Akad. Nauk SSSR*, *233*, 316–319, 1977 (in Russian).
- Kerr, R. A., Tracing the wandering poles of ancient Earth, *Science*, *236*, 147–148, 1987.
- Khramov, A. N., Paleomagnetism and problems of geotectonics, *Tectonosphere of the Earth*, Nauka, Moscow, 1978 (in Russian).
- Khramov, A. N., Standard sequences of paleomagnetic poles from North Eurasia plates: Implications for paleogeodynamic problems on the territory of the USSR, *Paleomagnetism and paleogeodynamics of the territory of the USSR*, pp. 135–149, VNIGRI, Leningrad, 1991 (in Russian).
- Khramov, A. N., Goncharov, G. I., Komissarova, R. A., et al., *Paleomagnetology*, Nedra, Leningrad, 1982 (in Russian).
- Khramov, A. N., and Kravchinskii, A. Ya., Geomagnetic and geotectonic cyclicity, *Papers of the 27th International Geological Congress, vol. 8, Geophysics*, pp. 161–169, Nauka, Moscow, 1984 (in Russian).
- Kirschvink, J. L., and Rozanov, F. Yu., Magnetostratigraphy of lower Cambrian strata from the Siberian platform: a palaeomagnetic pole and a preliminary polarity time-scale, *Geol. Mag.*, *121*, 189–203, 1984.
- Kirschvink, J. L., Ripperdan, R. L., and Evans, D. A., Evidence for a large-scale reorganization of Early Cambrian continental masses by inertial interchange true polar wander, *Science*, *277*, 541–545, 1997.
- Kiselev, V. I., and Aparin, V. P., *Evolution of the Earth-Moon system and geodynamic processes in the Phanerozoic*, IF SO AN SSSR, Krasnoyarsk, 1987 (in Russian).
- Klewin, K. W., and Berg, J. H., Geochemistry of the Maimense Point volcanics, Ontario, and implications for the Keweenawan paleomagnetic record, *Can. J. Earth Sci.*, *27*, 1194–1199, 1990.
- Klootwijk, C. T., Review of Indian Phanerozoic palaeomagnetism: implications for the India-Asia collision, *Tectonophysics*, *105*, 331–353, 1984.
- Komissarova, R. A., Iosifidi, A. G., and Khramov, A. N., Geomagnetic reversals recorded in a section of the Late Riphean Katav Formation, South Urals, *Fiz. Zemli*, (2), 60–68, 1997 (in Russian).
- Kono, M., and Tanaka, H., Mapping the Gauss coefficients to the pole and the models of paleosecular variation, *J. Geomagn. Geoelectr.*, *47*, p. 115, 1995.
- Kravchinskii, A. Ya., *Paleomagnetic and paleogeographic reconstructions of Precambrian platforms*, Nedra, Moscow, 1977 (in Russian).
- Kravchinskii, A. Ya., *Introduction into geohistorical prediction*, Nauka, Novosibirsk, 1987 (in Russian).

- Larson, R. L., Geological consequences of superplumes, *Geology*, *19*, 963–966, 1991.
- Larson, R. L., and Olson, R. L., Mantle plumes control magnetic reversal frequency, *Earth Planet. Sci. Lett.*, *107*, 437–447, 1991.
- Lin, J. L., Fuller, M., and Zhang, W. Y., Paleogeography of the North and South China blocks during the Cambrian, *J. Geodynam.*, *2*, (213), 91–114, 1985.
- Loper, D., Mantle plumes, *Tectonophysics*, *187*, 373–384, 1991.
- Loper, D., and McCartney, K., Mantle plumes and the periodicity of magnetic reversals, *Geophys. Res. Lett.*, *13*, 1525–1528, 1986.
- Loper, D., McCartney, K., and Busina, G., A model of correlated episodicity in magnetic field reversals, climate and mass extinctions, *J. Geol.*, *96*, 1–15, 1988.
- Marzocchi, W., Mulargia, F., and Paruolo, P., The correlation of geomagnetic reversals and mean sea level in the last 150 Myr, *Earth Planet. Sci. Lett.*, *1*, 383–393, 1992.
- Marzocchi, W., and Mulargia, F., The periodicity of geomagnetic reversals, *Phys. Earth Planet. Inter.*, *73*, 222–228, 1992.
- McElhinny, M., Geomagnetic reversals during Phanerozoic, *Science*, *172*, 157–159, 1971.
- McElhinny, M. W., and Lock, J., Global paleomagnetic database project, *Phys. Earth Planet. Inter.*, *63*, 1–6, 1990.
- McElhinny, M. W., and Lock, J., Global paleomagnetic database supplement number one, update to 1992, *Surv. Geophys.*, *14*, 303–329, 1993.
- McElhinny, M. W., and McFadden, P. L., Paleosecular variation over the past 5 Myr based on a new generalized database, *Geophys. J. Int.*, *131*, 240–252, 1997.
- McElhinny, M. W., McFadden, P. L., and Merrill, R. T., The time-averaged paleomagnetic field 0–5 Ma, *J. Geophys. Res.*, *101*, 25,007–25,027, 1996.
- McFadden, P. L., and Merrill, R. T., Lower mantle convection and geomagnetism, *J. Geophys. Res.*, *89*, 3354–3362, 1984.
- McFadden, P. L., and Merrill, R. T., Geodynamo energy source constraint from paleomagnetic data, *Phys. Earth Planet. Inter.*, *43*, 22–33, 1986.
- McFadden, P. L., Merrill, R. T., and McElhinny, M. W., Dipole/quadrupole family modeling of paleosecular variation, *J. Geophys. Res.*, *93*, 11,583–11,588, 1988.
- McFadden, P. L., and Merrill, R. T., Asymmetry in the reversal rate before and after the Cretaceous Normal Polarity Superchron, *Earth Planet. Sci. Lett.*, *149*, 43–47, 1996.
- Meert, J. G., and Van der Voo, R., Palaeomagnetic and $^{40}\text{Ar}/^{39}\text{Ar}$ study of the Sinyai dolerite, Kenya, Implications for Gondwana assembly, *J. Geol.*, *104*, 131–142, 1996.
- Merrill, R. T., and McElhinny, M. W., *The Earth's magnetic field*, Acad. Press, London, 1983.
- Mikhailova, N. P., Kravchenko, S. N., and Glevasskaya, A. M., *Paleomagnetism of anorthosites*, Naukova dumka, Kiev, 1994 (in Russian).
- Mikhailova, N. P., Kravchenko, S. N., and Glevasskaya, A. M., Paleotectonic analysis of ancient magnetization directions from autonomous anorthosite of East Siberia, *Geofiz. Zh.*, *18*, 3–16, 1996 (in Russian).
- Molostovskii, E. A., Pevzner, M. A., Pechersky, D. M., Rodionov, V. P., and Khramov, A. N., Phanerozoic magnetostratigraphic scale and geomagnetic reversal recurrence, *Geomagn. Issledov.*, (17), pp. 45–52, Nauka, Moscow, 1976 (in Russian).
- Molostovsky, E. A., and Khramov, A. N., Paleomagnetic scale for the Phanerozoic and magnetostratigraphic problems, *Proc. 27 Inter. Geol. Congress, vol. 1*, Nauka, Moscow, 1984.
- Negi, J. G., and Tiwari, R. K., Matching long-term periodicities of geomagnetic reversals and galactic motions of the Solar system, *Geophys. Res. Lett.*, *10*, 713–716, 1983.
- Opdyke, N. D., and Divenere, V. J., Paleomagnetism and Carboniferous climate, *US Geol. Surv. Bull.*, (2110), 8–10, 1995.
- Oppenheim, M. J., Piper, J. D. A., and Rolph, T. C., A palaeointensity study of Lower Carboniferous transitional field directions, the Cockermouth lavas, northern England, *Phys. Earth Planet. Inter.*, *82*, 65–74, 1994.
- Osipova, E. P., Rodionov, V. P., and Khramov, A. N., Paleomagnetic stratigraphy of the Precambrian, *Geomagnetism, Theoretical and applied aspects*, pp. 126–135, Naukova dumka, Kiev, 1988 (in Russian).
- Panella, G., Paleontological evidence on the Earth's rotational history since early Precambrian, *Astrophys. Space Sci.*, *16*, p. 212, 1972.
- Park, J. K., Buchan, K. L., and Harlan, S. S., A proposed giant radiating dyke swarm fragmented by the separation of Laurentia and Australia based on paleomagnetism of 780 Ma mafic intrusions in western North America, *Earth Planet. Sci. Lett.*, *132*, 129–139, 1995.
- Park, J. K., and Gower, C. F., Paleomagnetism of pre-Grenvillian mafic intrusions from the northeast Grenville Province, Labrador: implications for the Grenville Track, *Can. J. Sci.*, *33*, 746–756, 1996.
- Pavlov, V. E., Burakov, K. S., Tselmovich, V. A., and Zhuravlev, D. Z., Paleomagnetism of sills in the Uchur-Mai area and intensity estimate of the Late Riphean geomagnetic field, *Fiz. Zemli*, (1), 92–101, 1992 (in Russian).
- Pavlov, V., and Gallet, Y., Upper Cambrian to Middle Ordovician magnetostratigraphy from the Kulumbe river section (northwestern Siberia), *Phys Earth Planet. Inter.*, *108*, 49–59, 1998.
- Perrin, M., and Shcherbakov, V., Paleointensity of Earth's magnetic field for the past 400 Ma: evidence for a dipole structure during the Mesozoic low, *J. Geomagn. Geoelectr.*, *49*, 601–614, 1997.
- Pesonen, L. J., Nevanlinna, H., Leino, M. A. H., and Ryno, J., The Earth's magnetic field maps of 1990, *Geophysica*, *30*, 57–77, 1994.
- Petrova, G. N., Hierarchy of characteristic times of geomagnetic field variations, *Dokl. Akad. Nauk SSSR*, *308*, 1346–1350, 1989 (in Russian).
- Petrova, G. N., and Pospelova, G. A., Excursions of the magnetic field during the Brunhes chron, *Phys. Earth Planet. Inter.*, *63*, p. 135, 1990.
- Petrova, G. N., Nechaeva, T. B., and Pospelova, G. A., *Characteristic changes in the geomagnetic field in the past*,

- Nauka, Moscow, 1992 (in Russian).
- Pechersky, D. M., *Petromagnetism and paleomagnetism*, Nauka, Moscow, 1985 (in Russian).
- Pechersky, D. M., Latitude dependence of summary amplitude of geomagnetic direction paleovariations in the Neogaea, *Geomagn. Aeron.*, *36*, 130–136, 1996 (in Russian).
- Pechersky, D. M., Some characteristics of the geomagnetic field over 1700 Myr, *Fiz. Zemli*, (5), 3–20, 1997 (in Russian).
- Pechersky, D. M., Comparison between the geomagnetic field behavior and variation rates of the organic world in the Neogaea, *Geomagn. Aeron.*, 1999, in print (in Russian).
- Pechersky, D. M., Neogaeon variations in the paleointensity and other characteristics of the paleomagnetic field, *Geomagn. Aeron.*, (3), 1998 (in Russian).
- Pechersky, D. M., and Nechaeva, T. B., Variations in the direction and intensity of the geomagnetic field in the Phanerozoic, *Geomagn. Aeron.*, *28*, 820–824, 1988 (in Russian).
- Pechersky, D. M., and Didenko, A. N., *Asian paleocean: Petromagnetic and paleomagnetic constraints on its lithosphere*, OIFZ RAN, Moscow, 1995 (in Russian).
- Pechersky, D. M., Reshetnyak, M. Yu., and Sokolov, D. D., Fractal analysis of the geomagnetic polarity time scale, *Geomagn. Aeron.*, *37*, 132–142, 1997 (in Russian).
- Piper, J. D. A., The paleomagnetism of middle Proterozoic dike swarms of the Gardar Province and Mesozoic dikes in SW Greenland, *Geophys. J. Int.*, *120*, 339–355, 1995.
- Pisarevsky, S. A., Gurevich, E. L., and Khramov, A. N., Palaeomagnetism of Lower Cambrian sediments from the Olenek River section: palaeopoles and the problem of magnetic polarity in the Early Cambrian, *Geophys. J. Int.*, *130*, 746–756, 1997.
- Radhakrishna, T., and Joseph, M., Proterozoic palaeomagnetism of the mafic dyke swarms in the high-grade region of southern India, *Precamb. Res.*, *76*, 31–46, 1996.
- Radhakrishna, T., and Mathew, J., Late Precambrian (850–800 Ma) palaeomagnetic pole for the south Indian shield from the Harohali alkaline dykes: geotectonic implications for Gondwana reconstructions, *Precamb. Res.*, *80*, 77–87, 1996.
- Rampino, M. R., Geomagnetism, sea level and tectonics, *Phys. Today*, pp. 120–122, Jan., 1988.
- Rampino, M. R., and Caldeira, R., Major episodes of geologic change: correlations, time structure and possible causes, *Earth Planet. Sci. Lett.*, *114*, 215–227, 1993.
- Richards, M. A., Duncan, R. A., and Courtillot, V. E., Flood basalts and hot-spot tracks: plume heads and tails, *Science*, *246*, 103–107, 1989.
- Ricou, L., and Gibert, D., Le sequence des inversions magnetiques analysee par ondelettes: un enregistrement de l'histoire tectonique du globe au toit du noyau, *C. R. Acad. Sci.*, *325*, 753–759, 1997.
- Sabadini, R., and Yuen, D. A., Mantle stratification and long-term polar wander, *Nature*, *339*, 373–375, 1989.
- Saradeth, R., Soffel, H.C., Horn, P., et al., Upper Proterozoic and Phanerozoic pole positions and potassium-argon ages from the East Sahara craton, *Geophys. J.*, *97*, 209–221, 1989.
- Seguin, M. K., and Zhai, Y., Paleomagnetic constraints in the crustal evolution of the Yangtze block, southeastern China, *Tectonophysics*, *210*, 59–76, 1992.
- Semikhatov, M. A., and Raaben, M. E., Variations in global diversity of Proterozoic stromatolites, 2. Africa, Australia, North America, and general synthesis, *Stratigr. Geol. Correlat.*, (1), 26–54, 1996 (in Russian).
- Shapiro, M. N., Pechersky, D. M., and Lander, A. V., On velocities and directions of absolute motions of subduction zones in the geological past, *Geotektonika*, (2), 3–13, 1997 (in Russian).
- Shibuya, H., Cassidi, J., Smith, I. E., and Itaya, T., Paleomagnetism of young New Zealand basalts and longitudinal distribution of paleosecular variation, *J. Geomagn. Geoelectr.*, *47*, 1011–1022, 1995.
- Smethurst, M. A., Khramov, A. N., and Torsvik, T. H., The Neoproterozoic and Paleozoic paleomagnetic data for the Siberian Platform: From Rodinia to Pangea, *Earth Sci. Rev.*, *43*, 1–24, 1998.
- Stacey, F. D., *Physics of the Earth*, Brookfield Press, Brisbane, 1992.
- Starunov, V. A., Iosifidi, A. G., and Sholpo, L. E., Paleomagnetic study of Paleozoic ophiolites in southern Mongolia, *Fiz. Zemli*, (1), 30–40, 1996 (in Russian).
- Tanaka, H., and Kono, M., Paleointensity database provides new resource, *EOS Trans. Am. Geophys. Un.*, *75*, p. 498, 1994.
- Tarling, D. H., and Abdeldayem, A. L., Palaeomagnetic-pole errors and “small-circle” assessment of the Gondwanan polar-wander path, *Geophys. J. Int.*, *125*, 115–122, 1996.
- Thomas, D. N., An integrated rock magnetic approach to the selection and rejection of ancient basalt samples for palaeointensity experiments, *Phys. Earth Planet. Inter.*, *75*, 329–342, 1993.
- Thomas, D. N., and Piper, J. D. A., Evidence for the existence of a transitional geomagnetic field recorded in a Proterozoic lava successions, *Phys. Earth Planet. Inter.*, *122*, 266–282, 1995.
- Thomas, D. N., Rolph, T. C., and Shaw, J., Palaeointensity results from the Permo-Carboniferous (Kiaman) reversed superchron: the Great Whin and Midland Valley sills of the northern United Kingdom, *Geophys. J. Int.*, *123*, 798–816, 1995.
- Torsvik, T. H., Smethurst, M. A., Van der Voo, R., Abrahamsen, N., and Halvorsen, E., Baltica. A synopsis of Vendian–Permian paleomagnetic data and their paleotectonic implications, *Earth Sci. Rev.*, *33*, 133–152, 1992.
- Trench, A., McKerrow, W., and Torsvik, T., Ordovician magnetostratigraphy: a correlation of global data, *J. Geol. Soc. Lond.*, *148*, 949–957, 1991.
- Tretyak, A. N., Vigilyanskaya, L. I., and Karzanova, A. Ya., Paleomagnetism of Vendian Ukraine (problem of boundary between the Precambrian and Phanerozoic), *Geofiz. Zh.*, *18*, (3), 36–45, 1996 (in Russian).
- Tsunakawa, H., Geomagnetic secular variation during the Brunhes epoch inferred from paleomagnetism and the last 200 years geomagnetic field, *J. Geomagn. Geoelectr.*, *40*, 1365–1385, 1988.
- Ueno, N., Geomagnetic paleointensity experiment on igneous and metamorphic rocks from Enderby Land in

- Napier complex, Antarctica, *Proc. NIPR Symp. Antarct. Geosci.*, 5, 193–200, 1995.
- Van der Voo, R., Paleozoic paleogeography of North America, Gondwana, and intervening displaced terranes: comparisons with paleoclimatology and biogeographical patterns, *Geol. Soc. Am. Bull.*, 100, 311–324, 1988.
- Van der Voo, R., Phanerozoic paleomagnetic poles from Europe and North America and comparisons with continental reconstruction, *Rev. Geophys.*, 28, 167–206, 1990.
- Van der Voo, R., True polar wander during the Middle Palaeozoic, *Earth Planet. Sci. Lett.*, 122, 239–243, 1994.
- Van der Voo, R., and Meert, J. G., Late Proterozoic paleomagnetism and tectonic models: a critical appraisal, *Precamb. Res.*, 53, 149–163, 1991.
- Van Fossen, M. C., and Kent, D. V., Paleomagnetism of 122 Ma plutons in New England and Mid-Cretaceous paleomagnetic field in North America: true polar wander or large-scale differential mantle motion? *J. Geophys. Res.*, 97, 19,651–19,661, 1992.
- Varygin, V. Yu., and Aparin, V. P., *Modulation of geomagnetic reversal frequency by eustatic sea level fluctuations*, IF SO AN SSSR, Krasnoyarsk, 1989 (in Russian).
- Vogt, P. R., Evidence for global synchronism in mantle plume convection and possible significance for geology, *Nature*, 240, 338–342, 1972.
- Vogt, P. R., Changes in geomagnetic reversals frequency at times of tectonic change: evidence for coupling between core and upper mantle, *Earth Planet. Sci. Lett.*, 25, 313–321, 1975.
- Williams, G. E., Resonances of the fluid core for a tidally decelerating Earth: cause of increased plume activity and tectonothermal reworking events? *Earth Planet. Sci. Lett.*, 128, 155–167, 1994.
- Witte, W. K., Kent, D. V., and Olsen, P. E., Magnetostratigraphy and paleomagnetic poles from Late Triassic–earliest Jurassic strata of the Newark basin, *Geol. Soc. Am. Bull.*, 103, 1648–1662, 1991.
- Wu, N., Fang, D., and Jin, G., Paleomagnetic features of middle Paleozoic rocks from western Zhejiang and southern Anhui, Yangtse plate, *J. Zhejiang Univ.*, 27, 199–207, 1993.
- Yanovskii, B. M., *Terrestrial magnetism*, LGU, Leningrad, 1978 (in Russian).
- Zhao, X., Coe, R.S., and Zhou, Y., New paleomagnetic results from north China: collision and suturing with Siberia and Kazakhstan, *Tectonophysics*, 181, 43–81, 1990.
- Zhao, X., Coe, R., Wu, Y., and Zhao, Z., Silurian and Devonian paleomagnetic poles from North China and implication for Gondwana, *Earth Planet. Sci. Lett.*, 117, 497–506, 1993.
- Zharkov, V. N., Karpov, P. B., and Leontjev, V. V., On the Thermal Regime of the Boundary Layer at the Bottom of the Mantle, *Phys. Earth Planet. Inter.*, 41, 138–142, 1985.
- Zonenshain, L. P., Kuz'min, M. I., and Kononov, M. V., Spatial reconstruction of continents in the Paleozoic and Mesozoic, *Geotektonika*, (3), 16–27, 1987 (in Russian).
- Zonenshain, L. P., Kuz'min, M. I., and Natapov, L. M., *Plate tectonics on the territory of the USSR, vols. 1 and 2*, Nedra, Moscow, 1990.

(Received May 15 1998.)